

NPS ARCHIVE  
1968  
YEHYA, M.

OXIDATION PROTECTION OF MOLYBDENUM  
BY DIVALENT METAL MOLYBDATES

by

Mohammed Akhtar Yehya



DUDLEY KNOX LIBRARY  
NAVAL POSTGRADUATE SCHOOL  
MONTEREY CA 93943-5101

# UNITED STATES NAVAL POSTGRADUATE SCHOOL



## THESIS

OXIDATION PROTECTION OF MOLYBDENUM  
BY DIVALENT METAL MOLYBDATES

By

Mohammed Akhtar Yehya

December 1968

*This document has been approved for public release and sale; its distribution is unlimited.*

LIBRARY  
NAVAL POSTGRADUATE SCHOOL  
MONTEREY, CALIF. 93940

OXIDATION PROTECTION OF MOLYBDENUM  
BY DIVALENT METAL MOLYBDATES

by

Mohammed Akhtar Yehya  
Commander, Pakistan Navy  
M.S.C. Patna University, 1944  
A.M.I.E.I., London

Submitted in Partial Fulfillment  
for the Degree of

MASTER OF SCIENCE IN MATERIAL SCIENCE

From the

NAVAL POSTGRADUATE SCHOOL  
December 1968

1968

YEHUA, M

## ABSTRACT

Ni and Mg molybdates were prepared by an aqueous process and identified by x-ray analysis. Differential Thermal Analysis (DTA) of molybdates and their solid solutions mixed at various proportions were carried out. The spalling of  $\text{NiMoO}_4$  on cooling was observed. This large exothermic phase transformation was modified. Flexural strength of  $\text{MgMoO}_4$  bars were determined. Furnace designed to carry out this test at elevated temperature Vacuum Stability of bars made of  $\text{MgMoO}_4$  at high temperatures was observed. Slurry process of coating Molybdenum was carried out with some success and the same sintered at  $950^{\circ}\text{C}$  in high vacuum. An attempt was made to study the coated material at high temperatures under high vacuum and desired controlled atmosphere by a metallograph.

TABLE OF CONTENTS

	<u>Page</u>	
I	INTRODUCTION	9
II	RECENT STUDIES	11
III	CRYSTALLOGRAPHY	18
IV	EXPERIMENTAL PROCEDURES	22
	1. Sample Preparation	22
	2. X-ray Powder Patterns	23
	3. $\text{MgMoO}_4$ - $\text{NiMoO}_4$ Solid Solutions	23
	4. Differential Thermal Analysis	23
	5. Fabrication Ceramic Bars	24
	6. Flexural Strength Measurements	24
	7. Hardness	25
	8. Vacuum Stability	25
	9. Shrinkage and Porosity	25
	10. Coatings	26
	11. Microscopic Studies of Oxide	28
V	RESULTS	30
	1. Spalling	30
	2. X-ray P. P.	32
	3. DTA	36
	4. Flexural Strength and Hardness	36
	5. Vacuum Stability	37
	6. Shrinkage and Porosity	39
	7. Coating	39
	8. Microscopic Studies	41
VI	CONCLUSIONS	42
VII	AREA OF OPPORTUNITY	43
	Bibliography	66



LIST OF ILLUSTRATIONS

<u>Figure</u>		<u>Page</u>
1	Strength Levels of Typical High-Temperature Structural Alloys	45
2	Changes in Oxidation Rate of Refractory Metals in Relation to Temperature	45
3	Summary of Published Results on Oxidation of Molybdenum Under Atmospheric Conditions	46
4	Oxidation of 20 MoFeNi alloys, 1000°C	46
5	Limits of Catastrophic Oxidation of Fe-Ni-Mo Alloys	47
6	Stability Relationships of Refractory Oxides	47
7	Ceramic Die Components, Vice and Clamps used for Molding Specimen	48
8	Assembled Die on the Hydraulic Press	48
9	Working Drawing of Ceramic Die	49
10	Center Point Micro Bending Fixture with Specimen as Assembled on Instron Tester	50
11	Two Point Micro Bending Fixture with Specimen as Assembled on Instron Tester	50
12	Working Drawing of Center Point Micro Bending Fixture	51
13	Working Drawing of Two-Point Micro Bending Fixture	52
14	Working Drawing of Split Furnace for Instron Machine	53
15	Redesigned Center-point Micro Bending Fixture Assembled on Instron Tester	54
16	Redesigned Two Point Micro Bending Fixture Assembled on Instron Tester	54
17	• View Showing Vacuum Stability Experiment Set-up	55
18	Working Drawing of Ohmic Heating Specimen	56
19	View of Uncoated and Coated Molybdenum Specimen	55
20	High Temperature Solid State Phenomenon Demonstrator	57
21	Thermogram of Nickel Molybdate	58

LIST OF ILLUSTRATIONS CONT'D

<u>Figure</u>		<u>Page</u>
22	Thermogram of Nickel and Magnesium Molybdates Solid Solution (3:1)	59
23	Thermogram of Nickel and Magnesium Molybdates Solid Solution (1:1)	60
24	Variation of Width with Temperature for Magnesium Molybdate Specimen Molded at 18500 psi	61
25	Variation of % Shrinkage with Temperature for Magnesium Molybdate Specimen Molded Under 18500 psi	62
26	Variation of % Loss in Weight with Temperature for Magnesium Molybdate Specimen Molded Under 18500 psi	63
27	Coated Surface of Specimen at 250°C	64
28	Coated Surface of Specimen at 900°C	65

#### ACKNOWLEDGEMENT

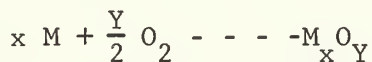
The research project reported here reflects the efforts and contributions of many people. The author wishes to express his appreciation for the encouragement, helpful advice and guidance of Dr. R. C. Carlston in the pursuit of this investigation. He is also greatful for suggestions of Professor J. R. Clark and Professor C. A. Hering which helped in x-ray data analysis and microscopic studies. The assistance of Mr. W. D. Roberts in designing the required equipment and data analysis proved invaluable. The vast amount of assistance received from Messers Don Clark, Roy Edwards, Bill Penprase, and Machine Facility is deeply appreicated. Also a well deserved thanks to Dr. G. F. Kinney, Professor G. D. Marshall and other members of the faculty and staff of Material Science and Chemistry Department for their understanding and encouragement during my studies in the Postgraduate School. The help of Dr. D. L. Douglas of Stanford Research Institute in clarifying the problems of high Temperature Materials Testing of metal oxides is appreciated.

Finally the completion of this work is due to the encouragement, patience and forbearance of my wife Ammatul Haye.



## INTRODUCTION

Neither a pure metal nor an alloy is thermodynamically stable in air even at ambient temperatures. The process of oxidation is an electron exchange reaction that produces when transfer occurs, a more stable electronic state for the atoms. Since the standard free energy of formation for all oxides except that of gold is exothermic, the oxidized state is the more stable state thermodynamically and thus oxidation is a spontaneous reaction:



The reaction path and the oxidation behaviour of a metal depends on a variety of factors and reaction mechanisms, hence may be complex. For a particular metal the reaction mechanism will in general be a function of heat treatment, temperature, surface preparation, gas composition, pressure, and duration of reaction (1). In view of the large variation in the properties of different metals and alloys and their oxides a very large number of theories are required to explain the oxidation behaviour of metals. (1,2,3,4)

As the temperature is increased, the instability of metal with respect to air increases. Most of the metals and alloys which are termed "oxidation resistant" have this quality by virtue of a thin protective oxide coating which rapidly forms on the surface and which prevents or retards the rate of further contact between air and metal. The service temperature of existing materials is limited by oxidation, and mechanical properties and melting point.

The development of jet engines, rapid advancement in rocket motor technology, nuclear energy applications and high velocity of aero-space vehicles have created demand of high-temperature structural material. The group of materials called refractory metals having a melting point higher than chromium 3405 F (1875 C) have been, during the last two decades, subjected to intensive research and development because of their high temperature strength properties. Figure 1 shows why refractory metals are best suited for structural application as compared to nickel and cobalt based alloys to meet high temperature requirements.

Rhodium, chromium, hafnium and perhaps iridium are the only refractory metals which are relatively oxidation resistant (5). The principal refractory metals like tungsten, tantalum, molybdenum and columbium do not form their own protective oxide coatings and hence suffer from drastic oxidation in air in the temperature range where their strength properties are required (Figure 2). Even though their melting points are 4000 F, they vigorously oxidize at temperatures above 1500 F. The oxide form usually sublime at these temperatures.

Two research approaches are available to overcome the disadvantages of poor oxidation resistance of refractory materials, one is the development of oxidation resistant alloys and the other is protective coatings. Extensive research has been carried out to improve the oxidation resistance of refractory metals by alloying. However improvement in oxidation resistance has been achieved at the expense of desirable mechanical properties (6). No satisfactory oxidation--resistant refractory metal alloy has been noted, and owing to the inherent properties of these metals and their oxides, the possibilities for developing such alloys do not appear promising except if some unique research alters

existing alloy concept. It is generally accepted that development of coating may solve the oxidation problem of structural refractory metal alloys. Thus emphasis is placed on development of coating system or systems to accomplish a desirable objective with a high degree of reliability.

A recent Navy Workshop on Materials (7) noted that the greatest obstacle to the general application of refractory metals is their poor resistance to oxidation at very high temperature. This research is in-part motivated by these findings.

One of the refractory materials possessing promising properties for use as high temperature construction and load bearing material is Molybdenum. Whereas mechanical properties of Molybdenum and its alloys are sufficient to meet severe stress requirements at elevated temperatures, it vigorously oxidizes at temperatures above 1500 F. Also in many proposed applications, pressure encountered may be much below atmospheric pressure. For example, in a hypothetical glide re-entry trajectory from 400,000 ft., the temperature at the stagnation point on leading edge surface may range from 2200 -- 4500 F at pressures of 0.01 to 500 mm Hg (5). Coatings have been developed to impart oxidation resistance from short duration at very high temperature to large duration at relatively lower temperature. This investigation was initiated with the specific objective to develop oxidation protection of Molybdenum using coating made of divalent metal molybdates ( $MMoO_4$ ).

#### RECENT STUDIES

The exact nature of the mechanism of the rate of oxidation of Mo has not yet been clearly established. One of the products of oxidation of Mo is Molybdc oxide ( $MoO_3$ ). It shows polymorphic transformation in

solid state and polymerisation in gaseous state. There is some evidence that overall rate and mechanism of oxidation of Mo are effected by the presence of structurally complex sub-oxides lying beneath the outer layer of  $\text{MoO}_3$ . Further once the oxide layer has been formed, the ability of oxidation reaction to continue depends on migration of at least one of the reactants (metal or oxygen atom) through this layer. A number of general references are available (1 - 7).

From the theoretical analysis of the oxidation of Molybdenum, Modisette and Schryer (8) obtained a rate equation which expresses oxidation rate as a function of temperature, gas properties, flow conditions and the activation energy at temperatures at which the oxide is gaseous. The oxidation rate was found to increase with increasing temperature, flow velocity and diffusivity in agreement with the result of analysis. The effect of temperature, pressure and mass flow on the oxidation of Molybdenum as summarized from published investigations of several workers (9,10,11,12,13,14) are shown in Figure 3.

LeChance and Jafee (15) observed that on oxidation of Nickel-clad Molybdenum even when the protective layer was consumed, a substantial protection of the substrate was provided by the resulting  $\text{NiMoO}_4$  scale. However, the scale spalled upon cooling to room temperature. On the surface of the residual Molybdenum base metal a scale of  $\text{MoO}_2$  was found by x-ray diffraction.

The effect of the additions of Molybdenum to Cobalt or Nickel on the oxidation rate and oxide structure at high temperature has been studied by Preece and Lucas (16). It was observed in both cases that additions upto 15% Mo produced an outer layer of monoxide ( $\text{CoO}$ ,  $\text{NiO}$ ) and subscale of Molybdate ( $\text{CoMoO}_4$ ,  $\text{NiMoO}_4$ ) and the latter spalled on cooling.

Brenner (17) has carried out systematic and complete work on the oxidation of Nickel-Molybdenum alloy at 1000 C. He observed that oxidation rate, which follows a parabolic law, increases upto 3 atomic % of Mo + W, then remains approximately constant upto 12 a.% beyond which it decreases again. Oxidation of the alloy produced three distinct layers. In addition to the external scale of NiO and NiMoO<sub>4</sub>, a subscale of MoO<sub>2</sub> is formed. At low concentration Mo and Ni ions migrate outward whereas O ions migrate inward. Ni ions from NiO which reacts with Mo at the NiMoO<sub>4</sub> interface forming MoO<sub>2</sub> and as its decomposition pressure is less than NiO, it precipitates into the alloy matrix. In the alloys containing upto 13.1% Mo the increase in oxidation rate is probably due to incorporation of some Mo ions in the NiO lattice. Being deficient in cations, ions of higher valency will introduce further vacancies in the nickel oxide structure thus increasing the rate of oxidation.

Migration of Ni ion across NiO layers is a controlling factor throughout oxidation process, as confirmed by small change in oxidation rates and heats of Activation of the alloys. At lower concentration of Mo the chief barrier is the NiO scale, above 13.1 at % the MoO<sub>2</sub> subscale becomes dense enough to impede migration of Ni ions and the rate therefore decreases. With upto 20 atomic % Mo, no catastrophic oxidation was observed.

Rathenau and Meijering (18) correlated the incidence of accelerated attack on various alloys with the formation and liquification of low melting or eutectic oxide mixtures. They suggest that rapid oxidation is not only caused by liquid oxides, but also it persists to continue further accelerated attacks. For chromium containing alloys the onset

of catastrophic oxidation occurs at about the temperature at which liquid molybdenum oxide dissolves  $\text{Cr}_2\text{O}_3$ .

Leslie and Fontana (19) studied the accelerated attack on several commercial alloys containing Mo. The oxides were found to have spinel type structure. The authors suggest that rapid oxidation was caused by the accumulation of gaseous  $\text{MoO}_3$  on the metal surface and the rate of oxidation is accelerated by the thermal dissociation of  $\text{MoO}_3$ .

Monkman and Grant (20) showed that accelerated (catastrophic) oxidation of steel caused by externally introduced vanadium pentoxide ( $\text{V}_2\text{O}_5$ ) depends on the external oxygen pressure and the process can be stopped if the pressure falls below a critical level. An outer layer of  $\text{Fe}_2\text{O}_3$  deposits, an inner layer of  $\text{Fe}_2\text{O}_3$  and  $\text{Fe}_3\text{O}_4$ , and a layer of  $\text{FeVO}_4$  between the metal-scale interface were observed. It is argued (21) that liquid  $\text{V}_2\text{O}_5$  carries the oxygen and oxides Fe to  $\text{Fe}_2\text{O}_3$  and transports the  $\text{Fe}_2\text{O}_3$  to a cooler solid oxide layer, and any resulting reduced Vanadium Oxide ( $\text{V}_2\text{O}_3$  with m.p. above  $1487^\circ\text{C}$  and  $\text{V}_2\text{O}_4$  with m.p.  $1545^\circ\text{C}$ ) is liquified only by oxidation to  $\text{V}_2\text{O}_5$ . This explanation is supported by the observation of Brasunas and Grant (22) that liquid  $\text{V}_2\text{O}_5$  dissolves a large amount of  $\text{Fe}_2\text{O}_3$  and that  $\text{Fe}_2\text{O}_3$  precipitates out from this solution upon cooling or upon reaching saturation.

As discussed earlier, Brenner (17) showed that binary Ni-Mo alloys up to 20.6 at % and binary Fe-Mo alloy up to 12.5 at %, do not oxidize catastrophically up to  $1000^\circ\text{C}$ . In both cases,  $\text{MoO}_2$  and molybdate in addition to  $\text{NiO}$  and  $\text{FeO}$  are formed during oxidation. Mo additions considerably decreases the oxidation rate of the iron alloy.  $\text{MoO}_2$  forms and separates  $\text{FeO}$  from metal base and thereby stops migration

of Fe ion and hence growth of FeO. Thus, even a few % of Mo reduces the oxidation of Fe sufficiently. Further studies of Brenner(23) indicate that when Ni or Cr is added to binary Fe-Mo alloy, catastrophic oxidation (of the same type found by Monkman and Grant) occurs in certain alloy concentration regions.  $\text{MoO}_2$  is formed immediately adjacent to the alloy surface. As long as the  $\text{MoO}_2$  is prevented from oxidizing to  $\text{MoO}_3$ , normal oxidation occurs. When, through pores and cracks formed by the stress relieving of the growing oxide layer, oxygen comes in contact with  $\text{MoO}_2$  layer, the latter is oxidized to molten or volatile  $\text{MoO}_3$ , and penetrates along the metal-oxide interface. Being more active, Fe and Cr reduce  $\text{MoO}_3$  to lower oxide releasing large amounts of heat.  $\text{MoO}_3$  being an excellent fluid, it probably dissolves the  $\text{Fe}_2\text{O}_3$  and  $\text{Cr}_2\text{O}_3$  oxides at the  $\text{MoO}_3$  metal interface. Heat of formation of Cr and Fe oxides further accelerate the fluxing. The dissolved oxide nucleate and precipitate again in the cooler region at the  $\text{MoO}_3$  liquid-solid oxide interface. The reduced Molybdenum oxide has continued access to oxygen and reoxidize to  $\text{MoO}_3$ .

Catastrophic oxidation at  $1000^{\circ}\text{C}$  was observed over a certain composition range (Figure 4). Between 15-35% Ni a liquid film of  $\text{MoO}_3$  is formed while outside this range Mo is prevented from oxidizing to the higher oxides. Brenner suggests that  $(\text{Fe},\text{Ni})_0 \cdot \text{Fe}_2\text{O}_3$  is more prone to cracking than pure  $\text{FeO} \cdot \text{Fe}_2\text{O}_3$ . Above 35% of Ni, the oxide formed may still crack, but alloy surface below the crack is sufficiently diluted with Ni to prevent formation of free  $\text{MoO}_2$ .

Gleiser et al. (24) have reported that when  $\text{NiMoO}_4$  and  $\text{Fe}_2\text{O}_3$  are heated together,  $\text{NiFe}_2\text{O}_4$  and  $\text{MoO}_3$  are formed implying that when Ni-Fe-Mo alloy is oxidized,  $\text{NiFe}_2\text{O}_4$  and  $\text{MoO}_3$  are formed in preference to

$\text{NiMoO}_4^*$  and  $\text{Fe}_2\text{O}_3$ . In  $20\text{Mo}20\text{Fe}60\text{Ni}$ , all the Fe will combine in  $\text{NiFe}_2\text{O}_4$ , next  $\text{NiMoO}_4$  will form and about 0.6 moles of Ni is left to oxidize to  $\text{NiO}$ . Thus, for this alloy at  $1000^\circ\text{C}$ , all oxides are solid and a low oxidation rate is expected. In case of  $20\text{Mo}40\text{Fe}40\text{Ni}$  alloy, similarly all the Fe combine to form  $\text{NiFe}_2\text{O}_4$ , all the Mo form  $\text{NiMoO}_4$  and about 0.1 mole of Ni is available for formation of  $\text{NiO}$ . However, in case of  $20\text{Mo}50\text{Fe}30\text{Ni}$  alloy, there is not enough Ni to tie up first all the Fe and then combine with Mo. Excess of Mo are free to form a liquid  $\text{MoO}_3$  layer and thus initiate catastrophic oxidation. The maximum amount of free  $\text{MoO}_3$  exists when all the Ni combines with all the Fe in  $\text{NiFe}_2\text{O}_4$ . This occurs at 27.56 w/o Ni. At lower percentage of Ni, Fe is in excess first forming  $\text{NiFe}_2\text{O}_4$  and then combining with Mo to form iron molybdate. Therefore the amount of free Mo is reduced as the percentage of Ni decreases (Figure 4). Larsen generalized to cover all Fe-Mo-Ni alloys as shown in Figure 5. Normal oxidation occurs in alloys which fall in sub triangle Fe-C-A or C-B-Ni. Catastrophic oxidation is expected in triangle A-C-Mo and C-B-Mo.

#### Chemical and Diffusion Compatibility of Coating Material and Substrate

Selection of material for coating depends on the substrate to be protected and the purpose and use of the same. At higher temperatures, the potential for different material to chemically react and interdiffuse increase, thereby the thickness of the substrate is reduced. Thermodynamics of a system for a given set of time-temperature and pressure conditions determine the direction in which a system has potential to go. Figure (5) shows the stability-relationship of refractory oxides as compiled by Kingery (25).

\*  $\text{NiMoO}_4$  is also unstable in contact with  $\text{Al}_2\text{O}_3$  dishes:  $\text{NiMoO}_4 + \text{Al}_2\text{O}_3 \rightarrow \text{MoO}_3 + \text{NiAl}_2\text{O}_4$  (21), the latter also has a spinel lattice and high Madelung Energy of the spinel lattice is sufficient to drive the metathetic reaction to the right.

Coating and substrate are considered as an integrated system. A good coating must be stable, should have no undesirable effect on mechanical properties of the substrate, should have closely matched thermal expansion to avoid cracking during thermal cycling, should accommodate creep and plastic deformation. In case of failure of the coating due to cracking, it should have self-healing properties. It should be easy to apply and if required, it should be able to stand impact, abrasion and erosion. Further, the rate of interdiffusion of coating and substrate should be slow compared to desired service life (1).

#### Coating for Molybdenum

##### Metal Base

Efforts to protect Mo turbine bucket using Ni-Cr, Ni or inconel in former years when temperature requirements were much lower than they are today, did not prove successful (26). Major shortcomings were large thermal expansion mismatch, rapid interdiffusion to form low melting eutectics or brittle intermetallics and relatively low maximum usable temperature. Platinum, rhodium, and their alloys have been considered as coatings for Mo. Shortcomings are thermal expansion mismatch, interdiffusion during longtime exposure and suspected diffusion of oxygen through Platinum to oxidize Mo and cause rupture of coating. Rhys (27) obtained a maximum life of 650 hours at 2190F with unbonded Platinum clad Molybdenum, whereas with an intermediate layer of alumina maximum life of 5,050 hours was observed. Platinum and rhodium are being investigated for high temperature short time application involving re-entry (5).

##### Silicide-Base Coatings

$\text{MoSi}_2$  may be considered as an intermetallic or hard metal. It has

long been recognized as an oxidation-resistant structural material and coating material for oxidation protection of Molybdenum metal (1,5,6,28). In low-stress conditions, it is amazingly oxidation resistant due to glassy protective  $\text{SiO}_2$  layer formed on the surface. Todd and Parry (29) suggest that a low melting mixture of  $\text{MoO}_2$  and  $\text{SiO}_2$  is formed initially, which flows and fills cracks before  $\text{MoO}_3$  volatilizes. Continuous coating of  $\text{MoSi}_2$  gives excellent resistance to oxidation, but any pin hole results in catastrophic oxidation at high temperature.

During oxidation,  $\text{MoSi}_2$  layer is consumed through oxidation and inward diffusion of Si, resulting in other intermetallic compounds,  $\text{Mo}_5\text{Si}_3$  and  $\text{Mo}_3\text{Si}$ . According to Perkins (30) the oxidation resistance decreases as  $\text{MoSi}_2 > \text{Mo}_5\text{Si} > \text{Mo}_3\text{Si}$ .

$\text{MoSi}_2$  coating at high temperature and reduced pressure loses its protectivity. Silicide coating which protected Mo for several hours at  $1650^\circ$  in air at atmospheric pressure failed in 15-30 minutes in air at 1 torr. At reduced pressure, it is considered that the attacks are localized and numerous pinholes are formed resulting in catastrophic oxidation (1,5,7).

In temperature range  $450-600^\circ\text{C}$ , the  $\text{MoSi}_2$  coated Mo rapidly disintegrates to a voluminous heap of powder. Fitzer (31) called this "silicide pest." This abnormal oxidation in which the protective scale fails to develop is a serious problem and needs further understanding of the reaction mechanism.

#### CRYSTALLOGRAPHY

Only as a result of some recent single crystal studies (32-37) have we arrived at any clear understanding of the crystal structure of the  $\text{MMoO}_4$  compounds for a small radius M ( $r \sim 0.9\text{\AA}$ ). The isomorphic character of the large cation  $\text{MMoO}_4$  and  $\text{MW}_2\text{O}_4$  compounds in the Scheelite structure

was discovered early in the development of crystal chemistry. There is no prior reason why the small cation molybdate and tungstates should not be isomorphic (38). The relationship was made clearer as a result of some research at Battelle (39) which showed that the molybdates (of unknown crystal structure) transformed at pressures 60 kbar at 900°C into the wolframite structure characteristic of most of the small M tungstates.

The most recent evidence (40) that both M and W cations are octahedrally coordinated with oxygen in alternating layers of a closely packed structure. Both atoms are displaced from the center of the octahedra. Some of the consequences of the structure are discussed by Rodier and Carlston (41) and by Ward (42).

The crystal structure of  $\text{CoMoO}_4$  (and isomorphic  $\text{NiMoO}_4$ ) was first discovered by Smith (32) and later elaborated on by Smith and Ibers (33). Although the true symmetry is monoclinic (Space group C2/m), there is a strong tetragonal pseudosymmetry because of a peculiarity in the relation between the reciprocal lattice parameters and the monoclinic angle. It should be possible to index powder patterns of  $\text{CoMoO}_4$  on the basis of this pseudostructure, but previous attempts to do this were unsuccessful (41). The structure is presently based rock salt lattice with 8/9th of the anion positions and 2/9th of the cation positions occupied. Although the octahedral cation coordination is maintained, the octahedron are distorted and reduced in size compared to  $\text{CoO}$ . Because the anion/cation ratio is 2, only half of the octahedral holes are filled. These chains of filled and open octahedra are parallel to the unique tetragonal axis. As in the wolframite structure, both cations are displaced from the center of their octahedra, the main difference in the structure lying in the packing sequence of octahedra and in the manner of sharing edges ( $\text{CoO}_6$  and  $\text{MoO}_6$  share edges,  $\text{NiO}_6$  and  $\text{WO}_6$  only share corners.)

Smith and Ibers (33) remark that they were unable to find any other isomorphic molybdates: The x-ray powder photographs of these molybdates Fe, Mg, Mn, and Zn all gave exceedingly complex patterns all different from each other." The situation has improved considerably due to the careful work of Abrahams on  $\text{MnMoO}_4$  (34),  $\text{ZnMoO}_4$  (36),  $\text{CuMoO}_4$  (37), and other related compounds.  $\text{MgMoO}_4$  and  $\text{MnMoO}_4$  are probably isomorphic (40). Although  $\text{MnMoO}_4$  is found to have the same monoclinic space group found for  $\text{CoMoO}_4$ , the lattice parameters are considerably different (see Table I) and the higher pseudosymmetry is not found. As a result the powder pattern of  $\text{MnMoO}_4$  gives a truer indication of the lower symmetry. The atom coordinates in the two structures also differ drastically: the  $\text{MnO}_6$  octahedra is almost undistorted, and the Mo cation is closer to distorted tetrahedral coordination. This change in coordination results in a 8% increase in volume per formula weight for  $\text{MnMoO}_4$ . Abrahams and Reddy (34) suggest that pressure may produce the following series of transformations:  $\text{MnMoO}_4$  str.  $\rightarrow$   $\text{CoMoO}_4$  str.  $\rightarrow$   $\text{NiWO}_3$  structure. Abrahams (36) has prepared a complete list of the metal ion coordination in the molybdates. This data is shown in Table II. There appears to be no clear basis in present-day crystal chemistry for explaining this array of structures.

Surprisingly, none of these studies made note of the spalling tendencies of  $\text{NiMoO}_4$  and (to some extent)  $\text{CoMoO}_4$  reported by Larsen (21, 24). These are presumably due to somewhat sluggish phase transformations. Larsen's crystallographic data is not consistent with the more recent studies, but is included in Table I for comparison. He also reported single crystal data on  $(\text{Mg}, \text{Co})\text{MoO}_4$ , but considering difference of coordination of the Mo cation in the two structure, little mutual solubility would be expected.

TABLE I  
Crystallographic Data on Monoclinic C2/m  
Molybdates

#	Compound	a(Å)	b	c	β	gm/cm <sup>3</sup>	Vol(Å <sup>3</sup> )	Z	Ref
1.	MgW <sub>4</sub> O <sub>4</sub>	4.68	5.66	4.92	89°.40'	5.66	130.30	2	34
2	NiW <sub>4</sub> O <sub>4</sub>	4.60	5.66	4.91	90°.5'	6.88	127.83	2	40
3	α MnMo <sub>4</sub> O <sub>4</sub>	10.47	9.52	7.14	106°.17'	4.18	683	8	31
4	α NiMo <sub>4</sub> O <sub>4</sub>	9.55	8.74	7.69	113°.45'	4.94	588	8	32
5	β MoMo <sub>4</sub> O <sub>4</sub>	9.70	9.16	6.69	107°.01'	5.11	568	8	21
6	α CoMo <sub>4</sub> O <sub>4</sub>	9.67	8.85	7.76	113°.49'	4.79	607	8	32
7	(Co,Mn)Mo <sub>4</sub> O <sub>4</sub>	10.22	9.303	7.04	106°.52'	4.08	632	8	21

TABLE II  
Coordination and Structure Type in Divalent-Metal  
Molybdates (DMo<sub>4</sub>O<sub>4</sub>)

Compound	Structure Type	D Coord.	M Coord.
CaMo <sub>4</sub> O <sub>4</sub>	Scheelite	8	4
BaMo <sub>4</sub> O <sub>4</sub>	Scheelite	8	4
SrMo <sub>4</sub> O <sub>4</sub>	Scheelite	8	4
PbMo <sub>4</sub> O <sub>4</sub>	Scheelite	8	4
MgMo <sub>4</sub> O <sub>4</sub> e	Wolframite	6	6
MnMo <sub>4</sub> O <sub>4</sub> e	Wolframite	6	6
FeMo <sub>4</sub> O <sub>4</sub> e, e	Wolframite	6	6
CoMo <sub>4</sub> O <sub>4</sub> e	Wolframite	6	6
NiMo <sub>4</sub> O <sub>4</sub> e	Wolframite	6	6
ZnMo <sub>4</sub> O <sub>4</sub> e, e	Wolframite	6	6
MgMo <sub>4</sub> O <sub>4</sub> i	MnMo <sub>4</sub> O <sub>4</sub>	6	4
MnMo <sub>4</sub> O <sub>4</sub> i	MnMo <sub>4</sub> O <sub>4</sub>	6	4
CoMo <sub>4</sub> O <sub>4</sub> i	CoMo <sub>4</sub> O <sub>4</sub>	6	6
NiMo <sub>4</sub> O <sub>4</sub> i	CoMo <sub>4</sub> O <sub>4</sub>	6	6
ZnMo <sub>4</sub> O <sub>4</sub>	ZnMo <sub>4</sub> O <sub>4</sub>	5 and 6	4

### Other Characterization Studies

Rodier and Carlston (41) have studied the thermogravimetric behavior of the molybdates. No evidence for loss or pick-up of oxygen could be found. Evidence of hydrates stable to 500°C were found. Van Uitert(43) studied the growth of single crystals by the Czochralski technique. He noted an inability to grow  $\text{NiMoO}_4$  crystals because of the spalling problem. The diffuse reflectance spectra of several molybdates has been determined (44). Because of the extreme distortion of the oxygen there may be little chance of analyzing the spectra in terms of crystal field splitting, as these authors have attempted. The same paper also gives the paramagnetic susceptibilities of the molybdates and observations on the results of solid-state reaction between the component oxides.

### EXPERIMENTAL PROCEDURES

#### 1. Sample Preparation

Aqueous solutions containing stoichiometric proportions of  $\text{MoO}_3$  and  $\text{NiCO}_3$  were evaporated in a beaker. The bulk was crushed and divided in three parts. Part One was labeled XA I, it was a hydrated form of  $\text{NiMoO}_4$ . Part Two was heated in a platinum dish to 450° for 24 hours in a heavy duty Muffle Furnace to dehydrate it, on cooling it was crushed to 100 mesh and labeled XA II. The third part was similarly heated to 650°C for 24 hours and after cooling crushed to 100 mesh and labeled XA III.

A small quantity of sample XA I was heated in a porcelain crucible at various temperatures for fixed durations and the appearance of the powder immediately upon removal, during and cooling to room temperature, was noted. The fractional weight losses during heating were recorded.

Next step was to mold a disc of  $\text{NiMoO}_4$  at 18,500 psi. Ethyl alcohol was used as a binder. 2-3 drops of alcohol per gram of powder

gave satisfactory results. Discs were molded both from sample XA II and XA III. The discs were dried overnight at room temperature and then heated in furnace at various temperatues upto 1050°C. The discs were allowed to cool inside the furnace and their appearance observed.

$\text{MgMoO}_4$  was similarly prepared by an aqueous process. Stoichiometric proportions of  $\text{MgO}$  and  $\text{MoO}_3$  were heated to evaporation. The bulk was crushed and heated to 450°C, cooled and crushed and heated to 450°C, cooled and crushed again to 100 mesh and labled as sample XB. A portion of this powder was heated to various temperature and change in appearance and fractional weight losses were recorded. Discs of  $\text{MgMoO}_4$  were also molded as described above and heated in furnace and physical changes recorded.

## 2. X-ray Powder Patterns

An x-ray diffraction pattern on  $\text{NiMoO}_4$  and  $\text{MgMoO}_4$  samples was obtained by using a Norelco diffractometer using traces of  $\text{NaCl}$  to provide reference d spacing. These patterns were then compared with published patterns (41).

## 3. $\text{MgMoO}_4$ - $\text{NiMoO}_4$ Solid Solutions

In view of instability of  $\text{NiMoO}_4$  reported (21), it was proposed to stabilize it by mixing with  $\text{MgMoO}_4$  in various proportions. Freshly prepared  $\text{NiMoO}_4$  and  $\text{MgMoO}_4$  were mixed in various proportions. Discs from some of these were molded, and heated to 800°C and cooled in furnace and change in surface conditions noted.

## 4. Differential Thermal Analysis (DTA)

Thermograms are obtained in the Du Pont Model 900 DTA by plotting temperature differential (Sample temperature minus reference temperature)

as a function of sample temperature. Thermograms of  $\text{NiMoO}_4$ ,  $\text{MgMoO}_4$  and mixture of two salts in various proportions were obtained.

### 5. Fabrication of Ceramic Bars

Because pure  $\text{NiMoO}_4$  could not be fabricated as bars due to spalling,  $\text{MgMoO}_4$  was then molded into bars. The mold with 0.2" x 2" recess was designed. However on molding it was found that the molded bar would crack on application of slight force to push it out. The mold was redesigned Figs. (7,8, and 9). No screws were used to hold the mold together. The mold parts could parts could be held together by small vice and clamps. Bars of  $\text{MgMoO}_4$  were molded at 18,500 psi in a Wabash Hydraulic Press. The samples could be removed after pressing without damage by loosening the vice and clamps. The molded bars were kept overnight at room temperature. To avoid warping the bars were turned 90 deg every 2 hours. After intial drying the specimens were placed in a drying oven at 100-110°C and further dried for 24 hours. Samples were then heated to various temperatures for a determined interval.

### 6. Flexural Strength Measurements

The molybdates are probably like most ceramics: they behave as brittle solids with little ductility and poor tensile strength. They are, however, strong in compression. Most ceramic strength measurements are based on flexural strength, the bending of a beam in center or two points loading as in Figs (10,11). Both methods are used extensively. Jigs were designed from stainless steel (Fig 12,13), to permit strength of the specimen to be determined at high temperature by the Instron machine. A furnace was designed (Fig. 14) to achieve heating of the specimen while under test. As the furnace could not be assembled in

time, the strength of the bars were determined at room temperature.

Difficulties were found in friction between the bar and points. The jig was redesigned Figs. (15,16).

#### 7. Hardness

Microhardness also has been used extensively as an indication of trends in strength of brittle solids. Our original aim was to carry out microhardness at elevated temperature, but it soon became apparent that it was beyond the state of the art for commercial equipment. The Vickers Hardness Number (VHN) was determined on sintered bars using the Wilson Tukon Tester available in the Department.

#### 8. Vacuum Stability

To observe stability of  $\text{MgMoO}_4$  at high temperature and low pressure conditions, the  $\text{MgMoO}_4$  bars previously heated to  $1000^{\circ}\text{C}$  were inserted in Vycor tube with one end closed which was connected to a diffusion vacuum system. The system consists of a roughing pump and an air cooled Veeco diffusion pump mounted on a rack with a valve manifold that permitted continuous operation of the diffusion pump even though the system was open. Pressure as low as  $10^{-7}$  torr could be achieved easily. The closed end of the Vycor tube was heated externally using a Hopkin's Electric Furnace. Temperature was recorded by a chromel-alumel thermocouple externally attached to the tube. This only gives an approximate indication of the temperature, Fig.(17).

#### 9. Shrinkage and Porosity Determination

ASTM C32-56 was followed in principle to determine the shrinkage of molded  $\text{MgMoO}_4$  bars at various temperatures. The width of the molded specimen was taken as reference. The measurement of width was carried out after heating the bars at various temperature for specified periods. Linear drying and firing shrinkages were calculated.

Apparent porosity, apparent specific gravity, bulk density of the bar heated at various temperatures were determined according to ASTM C-20(1961). Instead of water, Benzene was used as the medium.

#### 10. Coatings

To list the usefulness of  $MgMoO_4$  as a coating on molybdenum, sample of pure cast metal was obtained from Dr. M. Semchyschen, Climax Molybdenum. Strips of suitable size were cut out and specimens were prepared Figs. (17,18) for diffusion type coating as below:

- i) specimen corners and edges rounded by rounding and finishing surfaces on Emery Polish paper followed by diamond micro polishing.
- ii) vapour degreased in Carbon tetrachloride to remove oil and grease. Clean gloves used for handling the specimens afterwards.
- iii) rinsed thoroughly in water and dried.
- iv) pickled at room temperature for 2 minutes in a solution composed of  $HNO_3$ , HF and water in ratio of 3:2:2.
- v) rinsed thoroughly in cold running water.
- vi) washed in acetone, rinsed in Methyl Alcohol and air dried.
- vii) the dried specimens were kept in polythene bags.

There are large numbers of methods of application of coating presently used in industries, each method of application has certain advantages and disadvantages depending on the end application, substrate size and geometry and the experience of the operators involved. The commonly used methods are summarized (6).

- a) Electro depositon methods:-
  - i) Aqueous Solution
  - ii) Fused Salt
  - iii) Organic Solvents
  - iv) Electrophoresis
- b) Spraying methods: -
  - i) Oxyfuel spraying
  - ii) Arc plasma spraying
- c) Cladding methods:-
  - i) Roll cladding
  - ii) Gas pressure bonding
- d) Vapor desposition methods:-
  - i) Pack cementation technique
  - ii) Chemical and pyrolytic reaction
- e) Enamelling methods
- f) Vacuum metallising methods
- g) Hot dipping method:-
  - i) molten metals
  - ii) Selective freezing
  - iii) Fused salts
- h) Slurry method:-
  - i) Painting technique
  - ii) Trowelling technique
- i) Exothermic reaction methods

A prime consideration in coating technology is adherence. If the coating is not bounded with substrate, it will fail under stress such as thermal stressing, differential expansion and mechanical loading. The interface bonding may be due to mechanical locking, mutual wetting, chemical reaction expitaxial overgrowth or diffusion. King et al (48) have discussed this subject in detail.

To obtain the  $MgMoO_4$  coating on Mo substrate, the following processes were tried:

- a) Heating a pickled specimen of Mo packed in  $MgO$  at  $600^{\circ}C$ .
- b) Application of a Slurry of  $MgMoO_4$  in a suitable medium on pickled surface of Mo and sintering the same at  $900-950^{\circ}C$  at low pressure to obtain diffusion.

c) Vapour deposition of Mg on a pickled specimen of Mo.

10(a) Heating with Mgo

The pickled specimen of Mo was buried in dried MgO in a platinum basin and heated for 6 hours at 600°C in a Hevi-Duty furnace.

10(b) Slurry Process

In the absence of suitable equipment for spraying, the slurry process was selected for application of  $MgMoO_4$  coating on Mo. The process consists of blending coating composition particles (smaller than 325 mesh), suspending it in a liquid carrier to make a slurry and painting, dipping or spraying on the substrate. Liquid vehicle should satisfactorily hold the coating particles in suspension and must not decompose and react with either coating or substrate ( ).

The first coat was applied and allowed to air dry for 1 hour, then a second coat was applied and air dried for 24 hours. The slurry required thorough mixing before and during use to prevent the suspensions from setting out. The dried specimen was diffusion annealed at 950°C for 8 hours in a high vacuum  $10^{-6}$  torr (Figs. 18,19).

10(c) For Vapour Desposition of Mg.

On the molybdenum specimen, the CEC vacuum desposition equipment was used. After vapour deposition it was proposed to heat the sample at 600°C for 2 hours so as to form a layer of  $MgMoO_4$  by interaction of the metal oxides.

11 Microscopic Studies of Oxidation

High temperature solid state microscopic demonstrator assembled by the Office of Naval Research, Naval Training Device Center and subsequently modified by Kindig (46) was used to study the surface coated specimen at high temperature at varying low pressure conditions (Figs. 19,20).

This unit consist of Unitron, model B-11 metallograph, a Unitron vacuum heating stage and air cooled veeco diffusion pump and an auxillary roughing pump. As these pumps are mounted on a rack along with a valve manifold the diffusion pump can be operated continuously, even if the system is open. The system is capable of producing pressure as low as  $10^{-7}$  torr, which is sufficient for normal operation of the heating stage.

For microscopic observation of the specimen's coated surface at high temperature two methods were considered. First encapsulation of specimen in a given atmosphere and second heating the specimen by its own resistance in a controlled atmosphere.

Although the first method was more suitable, the equipment has certain limitations and this method was not found satisfactory by Kindig (46). Ohmic resistance has been previously used successfully by Brzustowski and Glassman (47). As the Ohmic resistance of Mo is low, the heating circuit was modified to give current density up to 125 amperes at 8 volts.

The heating stage consists of water-cooled stainless steel containers with a quartz window to permit observation of the specimen surface through the metallograph.

The specimens were specially prepared with coatings applied only in area under direct observation by microscope, this enabled a proper electric contact. The coated specimens were first sintered in quartz tube at 1108C and  $10^{-6}$  torr for 8 hours before observation in the metallograph. The metallograph was fitted with ROMIX rotary selector switch unit, a motion picture camera and a photo cell of light meter. A Tanack 35 mm focal plane camera can be simultaneously mounted.

Due to objective-specimen distance limitations, only two of the available objectives 5X, 10X could be used. For photographic method 10X, and 20X projection lenses could be used successfully, given magnification of 50X to 200X when used along with usable objectives. The magnification factor of 0.75X is achieved when Tanak 35 mm camera is used with Romix unit; this reduces the overall magnification by 25%.

## RESULTS

### 1. Spalling and Dehydration

a) Disc molded from XA II and XA III samples of  $\text{NiMoO}_4$  when heated upto  $1000^{\circ}\text{C}$  in the Muffle furnace remained stable with no crack or disintegration. However, during heating above  $700^{\circ}\text{C}$  "smoke" resembling  $\text{MoO}_3$  was given out. Some of the whiskers from this smoke which had condensed on the cooler part of the furnace were collected and identified by x-ray diffraction as  $\text{MoO}_3$ .

On cooling to  $290^{\circ}$  -  $310^{\circ}\text{C}$  discs of sample XA II disintegrated with explosive violence into fine powder giving out green white smoke. Discs from sample XA III also spalled and surface cracked, but with less violence and very little smoke. Larsen (21) determined a ratio of  $V_\alpha/V_\beta$  for  $\text{NiMoO}_4$  = 1.127 i.e., a volume change of 12.7% upon transformation. This suggests a possible phase transformation on cooling.

b) Considering x moles of water of crystallization and y moles of absorbed water associated with each mole of nickel molybdate. We have the molecular weight of starting material as  $218.64(\text{NiMoO}_4) + 18(x + y)$   $\text{H}_2\text{O}$  which on dehydration should become 218.64. Hence:

TABLE III

#	Temperature in centigrade	Time in hours	$\frac{W}{W_f}$	(x + y)	Hot	Color	Cold
1	200	6	0.05140	0.6250	lightgreen	lightgreen	
2	300	6	0.0726	0.8825	lightgreen	lightgreen	
3	400	6	0.1010	1.2253	tannishgreen	Pale gray green	
4	500	6	0.1065	1.2935	light tan	"	
5	600	6	0.1095	1.3300	brown	green	
6	700	6	0.1098	1.3320	brown	dark green	
7	800	6	0.1108	1.3450	brown	"	
8	900	6	0.1123	1.3654	brown	"	
9	1000	6	0.1117	1.3571	brown	olive green	

TABLE IV

#	Temperature in Centigrade	$\frac{W}{W_f}$	Time in hours
1	110	.00505	8
2	300	.00652	"
3	600	.00878	"
4	800	.0352	"
5	1000	.0467	"
6	1200	.0492	"

$$\frac{\text{final weight}}{\text{initial weight}} = \frac{W_f}{W_0} = \frac{218.64}{218.64 + 18(x + y)}$$

$$\text{ii} \quad x + y = \frac{218.64}{18} \left( \frac{W_0}{W_f} - 1 \right) = 12.15 \frac{\Delta W}{W_f}$$

The results are tabulated in Table III

c) Disc of  $\text{MgMoO}_4$  were also heated in a furnace upto  $1150^\circ\text{C}$ .

The discs remained dimensionally stable on heating and on cooling.

The color changed from white to light brown above  $900^\circ\text{C}$ , with specks of yellowish white spots (Fe impurity?)

d) The  $\text{MgMoO}_4$  sample X B was previously heated to  $450^\circ\text{C}$ . Known weights were heated in a crucible to various temperatures for fixed times in a muffle furnace and fractional loss in weight calculated as shown in Table IV.

e) Discs were molded containing  $\text{NiMoO}_4$  (X A II) and  $\text{MgMoO}_4$  (X B) in ratios of 3:1 and 1:1. These discs were heated to  $800^\circ\text{C}$ , on cooling both spalled. The first spalled at  $270^\circ\text{C}$  and shattered the disc with a little violence, wheras the second type spalled at  $250^\circ$  but developed surface cracks only.

## 2. X-ray Powder Pattern

Powder patterns from Cu k radiation were examined using a Norelco diffractometer. Recordings were made with the Scintillating counter sweeping from low Bragg angle towards high angle at the scanning rate of  $\frac{1}{2}^\circ(2\theta)$  per minute. The pattern from a silicon "standard" was first run as an internal standard for determining index error in scanning angle and a powder pattern of NaCl was then recorded for reference.

TABLE V

NiMoO<sub>4</sub> XA II

2θ	I	d	2θ	I	d
8.05	25	10.974	47.45	9	1.914
12.85	6	6.884	50.7	5	1.799
14.40	33	6.1460	53.4	7.5	1.714
19.10	8	4.643	56.25	6	1.634
23.45	5	3.791	56.75	7	1.621
24.05	9	3.697	57.15	5	1.611
25.45	17	3.497	57.75	8	1.595
25.8	19	3.450	58.10	8	1.586
28.20	6	3.1620	60.6	4	1.527
28.95	42	3.082	61.8	9	1.500
*31.8	16	2.812	62.2	8	1.491
32.65	17	2.740	63.8	6	1.458
38.65	7	2.328	64.7	5	1.439
39.10	14	2.302	66.3	7	1.409
41.3	8	2.184	67.05	6	1.395
44.0	20	2.056	67.65	6	1.384
			68.4	5	1.371

\*NaCl trace

TABLE VI

MgMoO<sub>4</sub>      XB

2θ	I	d	2θ	I	d
16.65	3	5.320	47.15	3	1.926
19.00	7	4.667	52.2	5	1.751
22.60	4	3.931	53.35	4	1.716
23.30	17	3.815	54.25	5	1.689
25.35	12	3.510	59.7	3	1.548
26.40	38	3.373	60.3	4	1.533
27.20	10	3.276	63.0	5	1.474
27.6	5	3.229	64.4	5	1.446
28.35	5	3.146	66.8	3	1.398
32.10	5	2.786			
*31.75	17	2.817			
33.70	4	2.657			
36.50	4	2.459			
38.70	4	2.323			
41.50	5	2.174			
43.5	3	2.079			
46.85	3	1.938			

\* NaCl trace

TABLE VII

(NiMoO<sub>4</sub> + MgMoO<sub>4</sub>) mixture 3:1

2θ	I	d	2θ	I	d
14.6	73	6.062	46.5	7	1.951
19.35	11	4.584	47.8	8	1.939
22.0	7	4.037	53.4	9	1.714
24.20	15	3.675	56.5	7	1.633
25.74	17	3.458	56.8	7	1.620
28.40	9	3.140	57.9	10	1.592
29.02	95	3.074	58.2	9	1.589
*31.65	30	2.825	62.0	10	1.496
32.9	16	2.728	63.8	7	1.458
33.1	18	2.704	66.6	8	1.403
36.6	6	2.453	67.1	7	1.394
39.0	8	2.3076	77.0	7	1.237
41.4	13	2.179			
43.4	7	2.083			*NaCl trace
44.0	42	2.056			
45.45	7	1.994			

Specimens were prepared by pressing the powdered molybdates with traces of NaCl in recessed sample holders.

Some powder from sample XA II was first heated to 800°C for 4 hours for complete dehydration. The data from powder pattern obtained is tabulated in Table V. It compares well with that of Carlston (41) and Larsen (21) and the sample was identified as  $\text{NiMoO}_4$ . On comparison with Carlston data (41) the data from powder pattern of XB sample was identified as that of  $\text{MgMoO}_4$ . The data is shown in Table VI.

The data, from a powder pattern of a mixture of XA II and XB samples, mixed in ratio of 3:1, is given in Table VII. It indicates a change in d-spacing and suggests the formation of a solid solution. None of the strong lines of  $\text{MgMoO}_4$  are present. However, the strong lines of  $\text{NiMoO}_4$  are present, but shifted towards smaller 'd' values.

### 3. Differential Thermal Analysis

The thermograms for  $\text{MgMoO}_4$  did not show any exothermic or endothermic fall or rise upto 800°C, both in heating and cooling cycles. The thermogram for  $\text{NiMoO}_4$  Fig. (21) showed a definite endothermic phase change at 700°C. On cooling from 850°C reverse change was observed at 775°C. Sharp exothermic peaks of large intensity was recorded at 305°C, followed by some small peaks.

Mixtures of  $\text{NiMoO}_4$  and  $\text{MgMoO}_4$  made in various proportions from 9:1 to 1:1 were also studied in D.T.A. Figs (22-23) indicate the stabilizing effect of  $\text{MgMoO}_4$  when mixed with  $\text{NiMoO}_4$  in ratio of 1:3 and 1:1.

### 4. Flexural Strength and Hardness

In the center point loading jig designed, the rectangular  $\text{MgMoO}_4$  (Fig. 12) bar was supported at the two knife edges and the load was applied at a single point at the center of the specimen Fig. (10). Two point-

loading system was also designed to achieve a constant bending moment at the center of the specimen. The jigs were assembled in the Instron machine with specimen. A furnace was designed to enclose the specimen and heat it to a desired temperature while under test (Fig. 14), however, it could not be produced in time for experimentation. The Transverse strength and Elastic modulus was determined at room temperature, using the following standard formulas:

$$\text{For center deflection } \max = \frac{3PL}{2bd^2}$$

$$E = \frac{PL^3}{4bd^3 Y}$$

$$\text{For 2 - point loading } \max = \frac{Pa}{bd^2}$$

$$E = \frac{Pa(3L^2 - 4a^2)}{2Ybd^3}$$

Table VIII contains the experimental data both for center point loading (#1 to 6) and 2-point loading (#7 to 12). The load cell used was 0-100 lb. A more accurate result could have been obtained if a lower range cell was available. To eliminate friction at the support and bearing, the jigs were redesigned. However, the results (not indicated here) were of the same order.

b) The Tukon Micro hardness test was carried out, but it was carried out, but it was observed that the molded bars and sintered bars cracked under load indicating that under present mode of preparation sufficient compactness was not achieved and due to porosity the specimen showed brittle behaviour.

## 5. Vacuum Stability

Molded bars of  $\text{MgMoO}_4$  were heated at  $950^{\circ}\text{C}$  in Vycor tube at a

TABLE VIII

#	Y in inches	b inches	d inches	p lb	max psi	$E \times 10^{-4}$ psi
1	.015	.218	.199	1.25	379	6.54
2	.010	.216	.198	1.30	404	10.45
3	.012	.228	.201	1.20	346	7.28
4	.013	.215	.204	1.25	367	7.15
5	.011	.226	.205	1.30	368	8.23
6	.012	.230	.203	1.40	390	8.23
7	.01	.195	.201	1.0	286	10.15
8	.012	.218	.195	1.0	272	8.34
9	.011	.234	.205	1.1	252	8.05
10	.012	.225	.204	1.25	298	8.88
11	.011	.220	.197	1.1	291	9.00
12	.010	.225	.202	1.25	306	10.68

# 1 to 6 center point loading  
 # 7 to 12 two point loading  
 $= 0.175$  in,  $a = 0.375$  in.

TABLE IX

#	Temperature in Centigrade	Time in hours	Width in inches	% Shrinkage	% loss in weight
1	20	24	0.2085	---	---
2	110	24	0.207	0.722	0.443
3	400	6	0.205	0.975	0.604
4	608	6	0.204	1.475	0.922
5	802	6	0.184	12.65	3.742
6	1001	6	0.177	16.93	4.580
7	1178°	6	0.176	17.60	4.833

pressure of  $2 \times 10^{-6}$  torr. There was almost no change in the weight of the specimens. The surface of the specimen looked smoother and the edges developed a bluish tinge indicating some reduction of Mo (VI)ion.

## 6. Shrinkage and Porosity

a) Of the three linear dimensions of the bar of  $\text{MgMoO}_4$ , the width was used for reference. The width of the specimen were measured at three positions. Five specimens were used. Linear drying and firing shrinkages were calculated as follows:

$$S_d = \frac{W_p - W_d}{W_d} \times 100$$

$$S_f = \frac{W_d - W_f}{W_f} \times 100$$

where  $W_p$ ,  $W_d$ ,  $W_f$  are plastic, dry and fired width of the specimen and  $S_d$  and  $S_f$  are the linear dry shrinkage and the linear firing shrinkage of the test specimen. Width, % shrinkage and % loss in weight have been plotted against temperature, Figs.(24-26) represent typical S-curves for ceramics. Results representing average values of each property are given in Table IX.

b) For determination of apparent porosity, water absorption, apparent specific gravity and bulk density ASTM C20-46 (1961) was followed. As  $\text{MgMoO}_4$  is soluble in water, Benzene was used instead. Dry weight D, suspended weight S, and saturated weight W of the specimen were measured. Specimens were heated for 6 hours at  $800^\circ$ ,  $1000^\circ$  and  $1200^\circ\text{C}$ . Five specimens were heated at each temperature. Results representing average values of each property are shown in Table X.

## 7. Coatings

a) Mo specimens were packed in dry  $\text{MgO}$  and heated to  $600^\circ\text{C}$  in Muffle Furnace for 6 hours on examination indicated excessive oxidation of substrate and formation of  $\text{MgMoO}_4$ . Further experimentation is

TABLE X

#	Temperature °C	App. Porosity P	App.		Sp. Gravity T	Bulk Density B
			Water A	Absorption A		
1	800°	16.38	6.09		3.298	2.72
2	1000°	2.39	0.638		3.680	3.59
3	1200°	2.14	0.605		3.690	3.60

required to establish the ideal temperature and duration of heating for Molybdate coatings.

b) Coating obtained by application of  $MgMoO_4$  suspended in mixture of Collodian and Butyle Acetate as vehicle, sintered for 8 hours at  $950^{\circ}C$  at  $10^{-6}$  torr was examined under a microscope. The surface was without any crack or discontinuity, but it was rough and contained a few pinholes which may have been formed by escaping vehicles.

On thermal cycling oxidation test, the coated specimen did not develop any defect or increase in weight up to  $450^{\circ}C$ . However, when heated to  $500^{\circ}C$  and cooled, the coating showed tendency to peel out, which may be indicative of either insufficient diffusion bonding attained by sintering at  $950^{\circ}C$  or thermal expansion mismatched between the coating and the substrate, a vacuum diffusion at  $1200^{\circ}C$  for 24 hours may produce a better bonding.

c) An attempt was made to vapor deposit Mg on the standard Mo strip. Unfortunately the vacuum evaporation equipment was set up for shadowing carbon replicas with Cr and it proved impossible to easily modify the holders for this operation.

#### 8. Microscopic Studies

Ohmic resistance heating specimens manufactured according to Fig. (18) were prepared, coated and sintered at  $950^{\circ}C$  for 6 hours at  $10^{-6}$  torr as described earlier. However, to ensure proper electric contact the coatings from the end portions were removed and surface properly cleaned. It was ensured that the area to be viewed directly by microscope has its coating intact. Once assembled in the heating stage, the temperature was monitored by means of chromel alumel thermocouple and displayed on Varian recorder as millivolts -- which

could be read in degrees by means of standard table. On heating to  $250^{\circ}\text{C}$  the specimen was observed to have developed circular drop-like pattern growth round nucleus --the pattern may be related to strains present, due to oxide particles (Fig. 27). For heating Mo specimen to higher temperature the specimen was redesigned to offer greater electric resistance at the central portion. Only this part of the specimen was coated and sintered at  $1100^{\circ}\text{C}$  at  $1 \times 10^{-6}$  torr for 12 hours in a quartz tube. This sample did not show any pin hole when viewed under a microscope. It could be heated to  $900^{\circ}\text{C}$  in the heating chamber with modified electric circuit using 8V-125 amps supply. Fig (25) shows the effect of heating on the specimen. It indicates further of oxide. The growing oxide may spall, as evidence by the crack in the upper right hand corner of Fig.(28). Because of the roughness of the surfacte, not much more detail is available at in Fig. (26).

#### VI CONCLUSIONS

1. The visual and DTA evidence clearly indicate a violent phase change on cooling  $\text{NiMoO}_4$  below  $300^{\circ}\text{C}$ . This microscopic change results in the observed shattering and smoking of processed pieces. It is not observed to that extent in free powder.

2. Addition of  $\text{MgMoO}_4$  moderates the phase change and lowers it in temperature, but even at 50 W %  $\text{MgMoO}_4$  the DTA indicates an exothermic process though of smaller magnitude. The powder pattern evidence indicate solid solution formation between  $\text{MgMoO}_4$  and  $\text{NiMoO}_4$  preserving the  $\text{NiMoO}_4$  structure.

3. Because of the porosity of the specimen , meaningful strength and hardness data could not be obtained. More sophisticated procedures such as hot pressing of specimen using agate dies at elevated

temperatures will be required.

4.  $\text{MgMoO}_4$  does not show any evidence of appreciable thermal disproportionation, even under vacuum conditions.

5. There was evidence that with increase in sintering temperature the quality of diffusion bonding could be improved. To obtain a better and even surface for microscopic study and improve bonding, hot spraying may prove effective.

6. Microscopic study of the surface was incomplete, a detail study is required under controlled atmosphere and elevated temperatures to study the changes that may take place on the coating surface under these conditions.

7.  $\text{NiMoO}_4$  is unstable as an oxidation resistant coating because of spalling. This seems to arrive from  $\beta \rightarrow \alpha$  phase transformation. (See Concl. #2) As spalling only occurs on cooling, solid solution of Ni and Mg molybdate may be useful as a one-shot coating to protect molybdenum on the heating cycle. The oxidation rate of molybdenum is sufficiently lower at  $300^{\circ}\text{C}$ , so that practical protection is achieved in the cycle of heating and cooling.

## VII AREA OF OPPORTUNITY

The brief time available for experimentation developed a number of areas which should be investigated further in order to really establish the feasibility of non-silicate protective coatings for molybdenum and its alloys. These would include: better ceramic fabrication facilities, higher temperature oven for sintering, single crystal studies, use of x-ray diffraction technique to follow structural changes in the coating after sintering, a more complete study of the pseudobinary  $\text{MgMoO}_4$  -  $\text{NiMoO}_4$ , use of more sensitive load cell for Instron tester, and development of more sophisticated coating facilities.

On a more fundamental plane there is a great need to know more about the factors which stabilize  $\text{MnMoO}_4$  on the one hand and lead to catastrophic phase transformation in  $\text{NiMoO}_4$  on the other. The crux of the matter seems to be the relative size of the ions (This line of reasoning is similar to that used in the classical studies of  $\text{ZrO}_2$  stabilized by  $\text{CaO}$  additions). One would expect however, that  $\text{Ni}^{++}$  and  $\text{Mg}^{++}$  would have about the same effective size in the molybdate, but the evidence seems to indicate  $\text{Ni}^{++}$  is appreciably smaller and distorts the expected regular octahedral coordination. Since Schwartz (39) found that  $\text{NiMoO}_4$  went through a phase transformation under pressure to the wolformite-structure, it should be possible to get the same type of transformation by chemical substitution in the  $\text{NiMoO}_4$  lattice.

In future studies some thought should be given to the actual practicality of providing protection for molybdenum at  $T > 2000^\circ\text{C}$ . More and more at these "low temperatures" the so called "super alloys" of Ni and Co are taking over roles formerly assigned to Mo. Super alloys have been developed with reasonable oxidation resistance, and with superior strength/weight ratio, so that the mission for Mo alloy will probably be at  $T > 2000^\circ\text{C}$ .

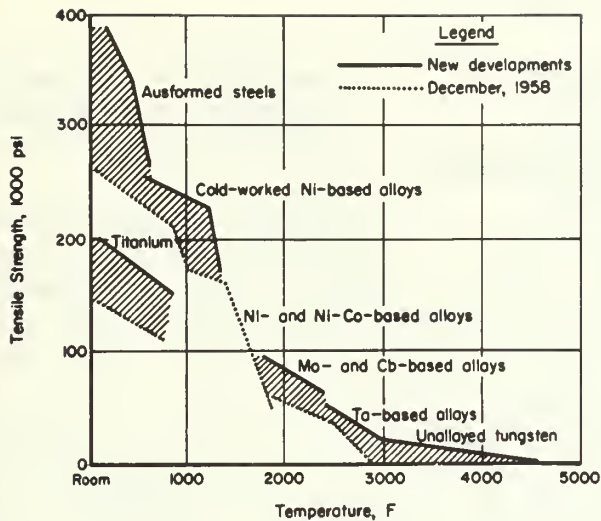


FIGURE 1

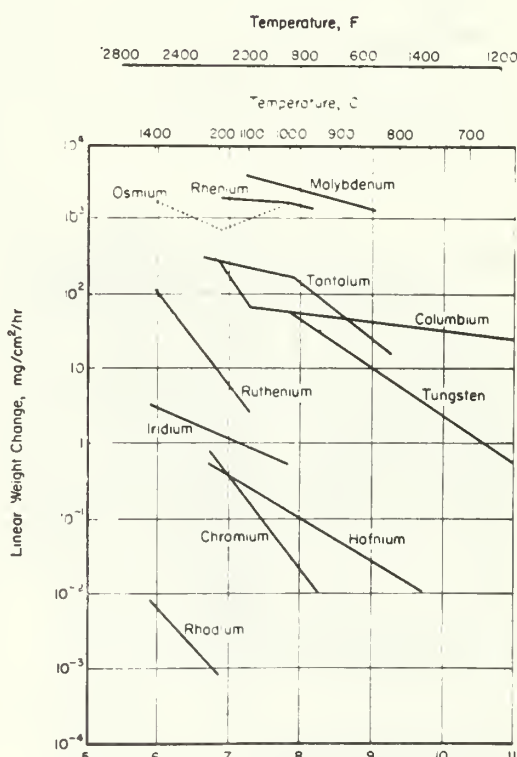
Strength Levels of Typical High-Temperature Alloys (49)

Shaded areas indicate the extent of the increase as measured by tensile strength

FIGURE 2

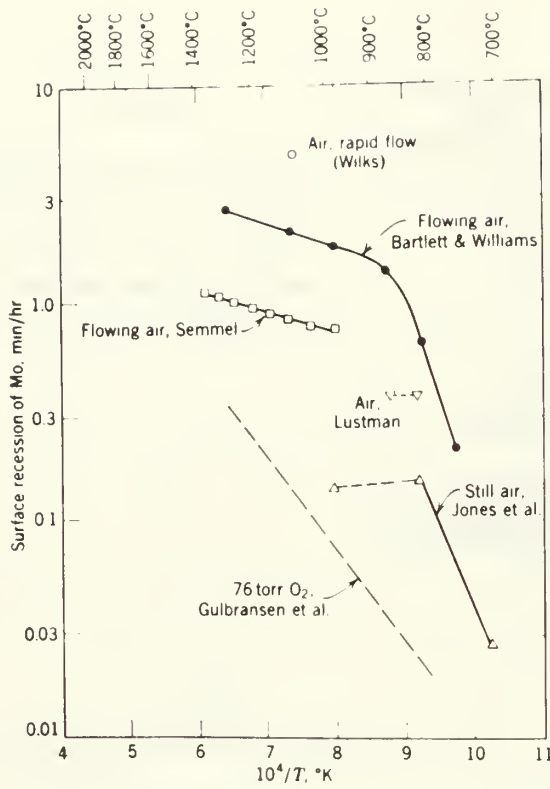
Changes in Oxidation Rate of Refractory Metals in Relation to Temperature (50)

Data for molybdenum, rhenium, osmium, ruthenium, iridium, and rhodium are weight-loss rates.



$$\text{Reciprocal Temperature } \frac{10^4}{T}, \text{ k}^{-1}$$

FIGURE 3



Summary of Published Results on Oxidation of Molybdenum under Atmospheric Conditions.

Surface recession rates as a function of  $1/T$ . Compiled by Per Kofstad (1) from results of several workers (9 - 14)

FIGURE 4

Oxidation of 20 Mo Fe Ni alloys, 1000°C (23)

(Nickel is substituted for iron in the original 20Mo80Fe alloys.)

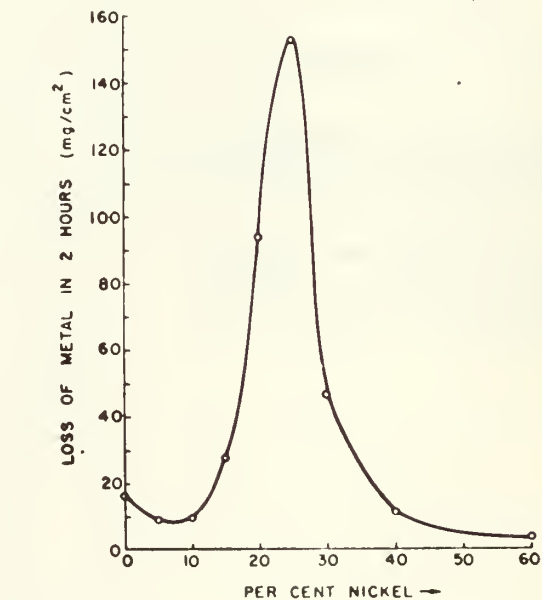
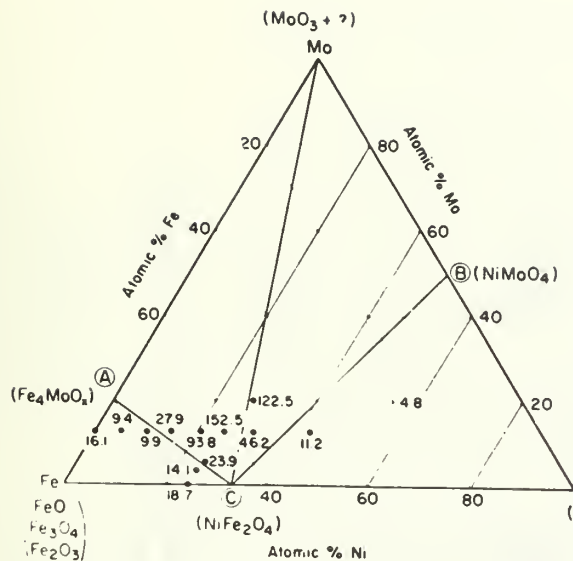


FIGURE 5



Limits of Catastrophic Oxidation of Fe-Ni-Mo Alloys (21).

FIGURE 6

Stability Relationships of Refractory Oxides (25).

Solid lines are lines of constant standard free energy of formation from the elements. The dark shadowed area is the region of greatest stability.

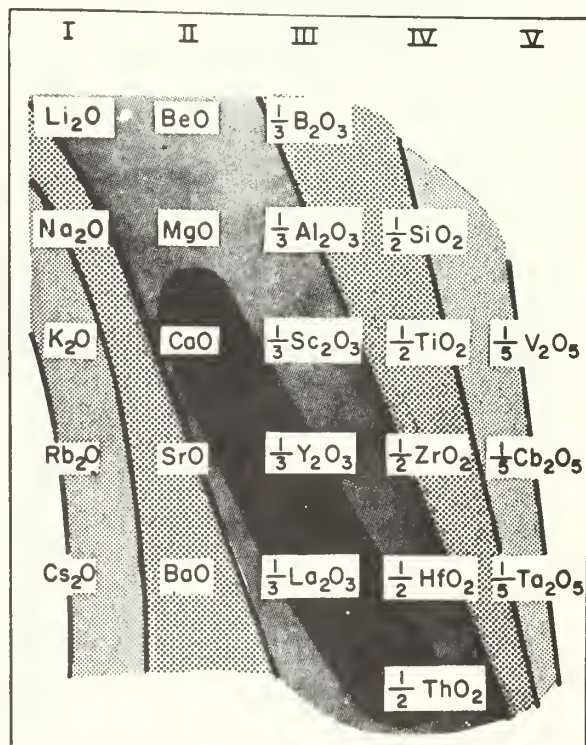




FIGURE 8  
Assembled Die on the Hydraulic Press.

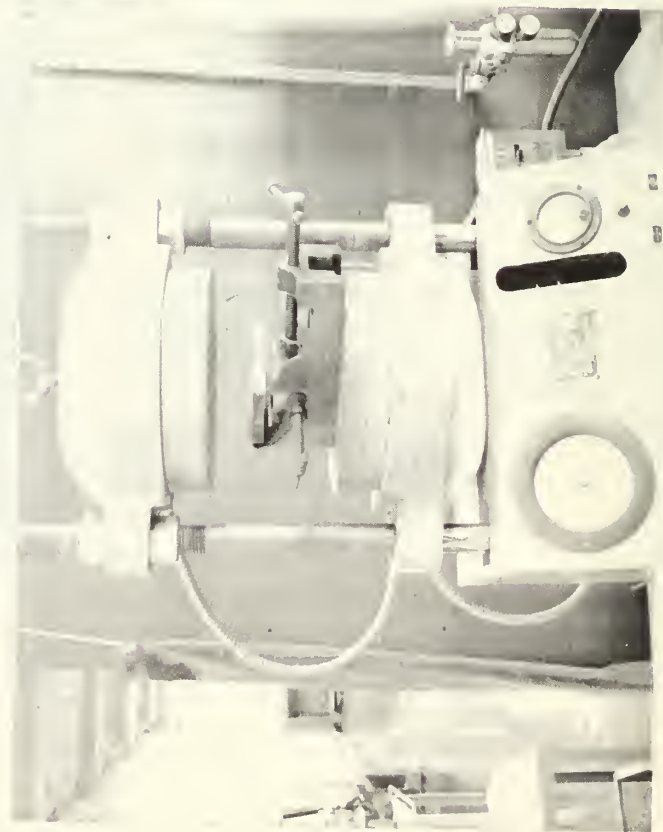
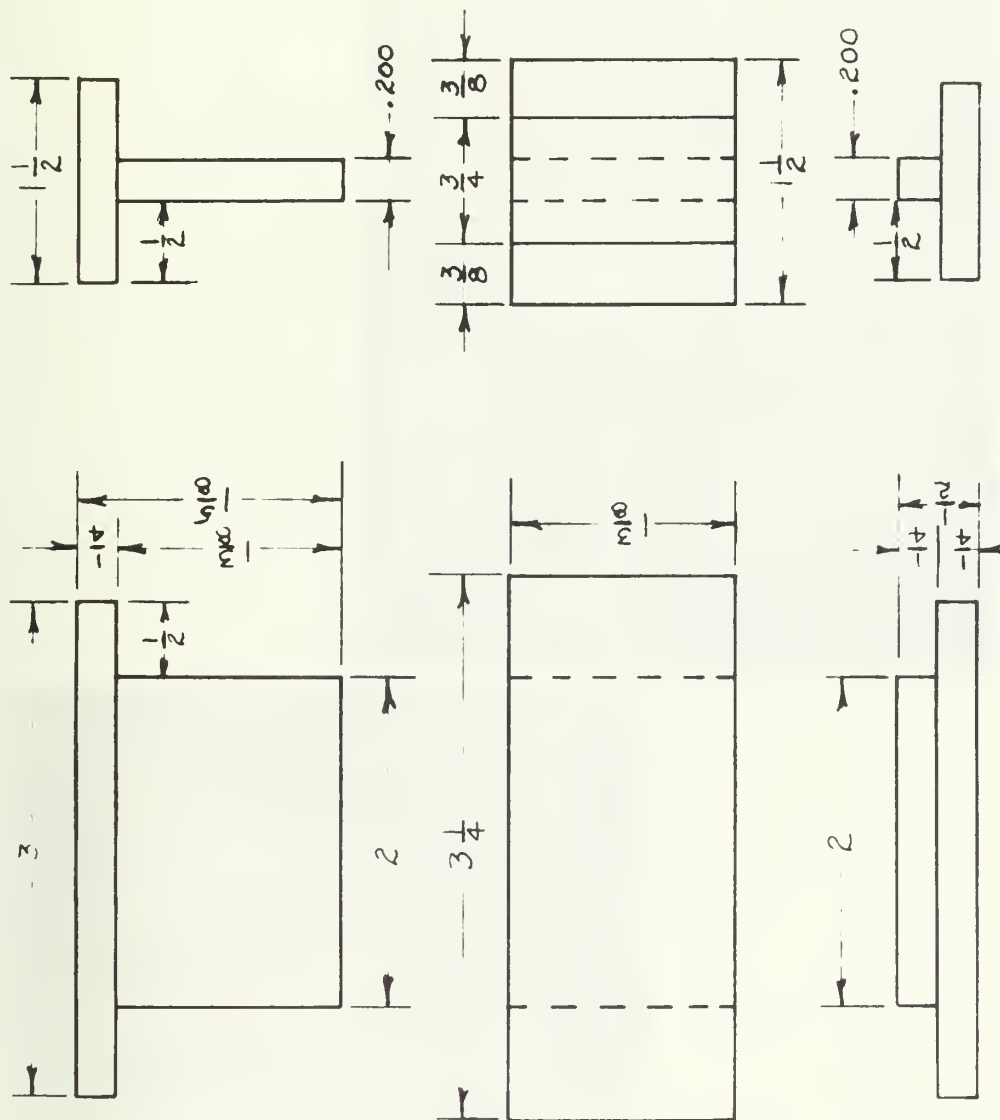


FIGURE 7  
Ceramic Die Components, Vice and Clamps Used for Molding the Specimen.



DRN. BY: B. R.

MATERIAL: DIE STEEL

SCALE: 1"-1"

CERAMIC DIE

DRN. BY: B. R.

FIGURE 9: Working Drawing of Ceramic Die

FIGURE 11

Two Point Micro Bending Fixture  
with Specimen as Assembled on  
Instron Tester

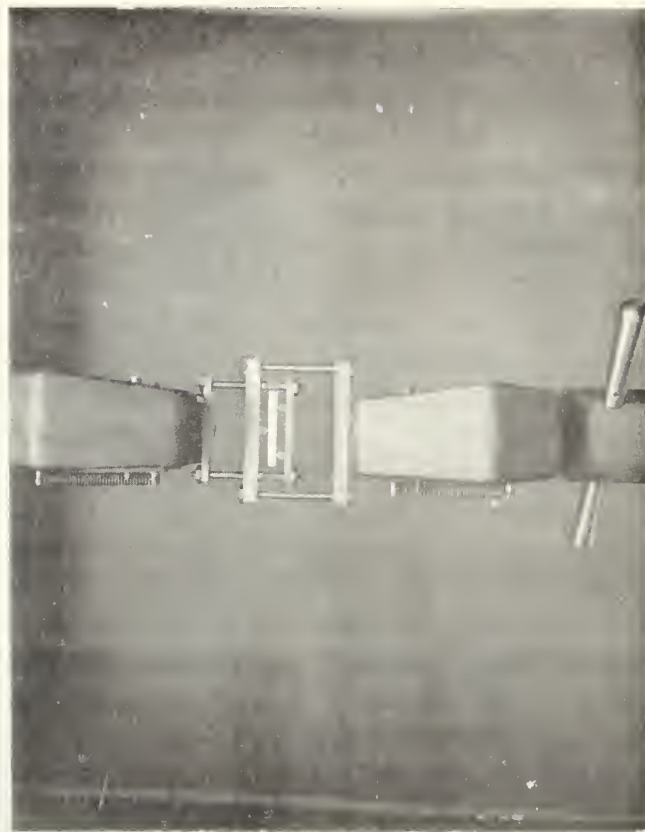
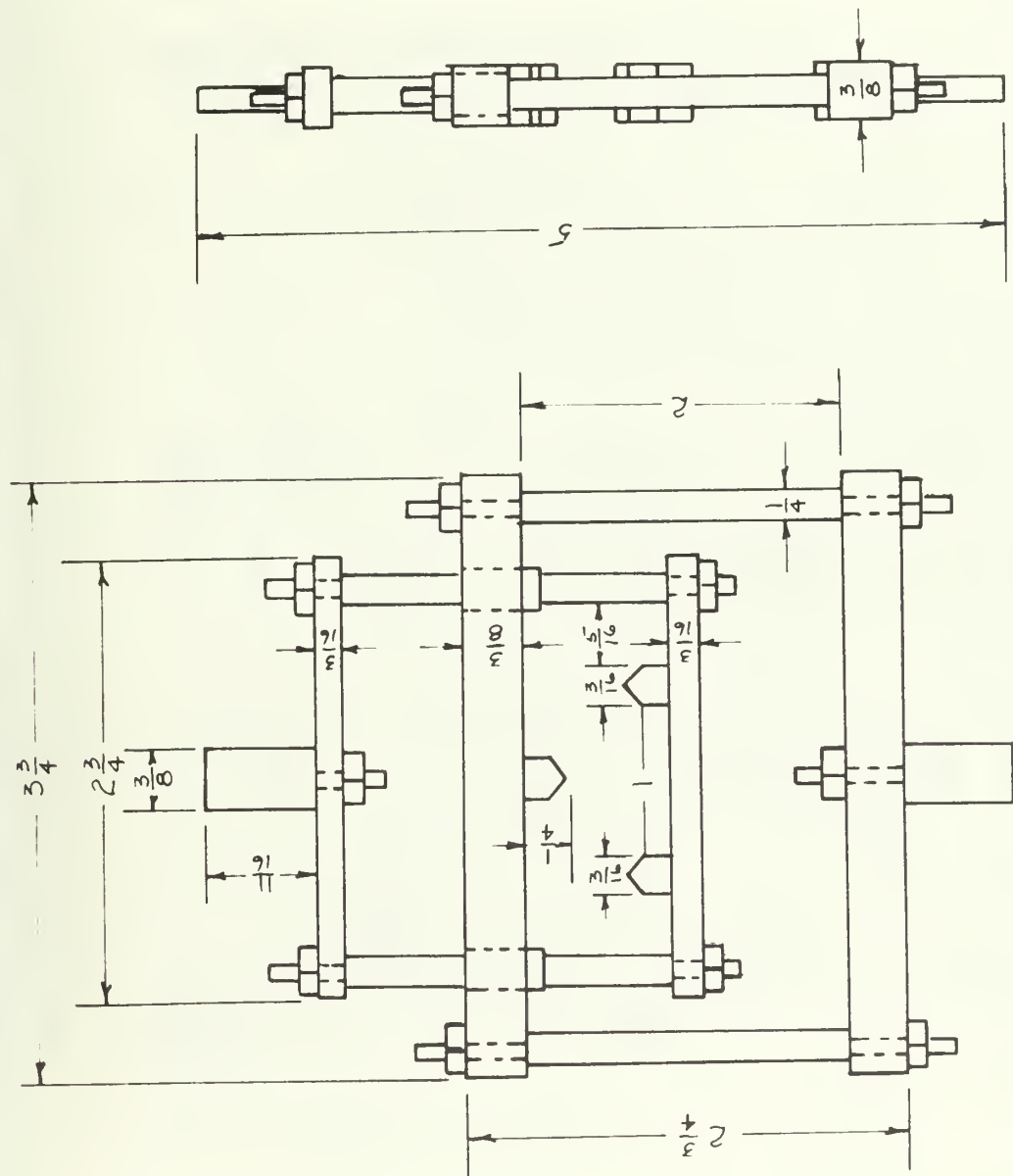


FIGURE 10

Center Point Micro Bending Fixture  
with Specimen as Assembled on Instron  
Tester





SCALE : 1" - 1"	MAT'L: C. R. STEEL	CTR. PT. MICRO BENDING FIXTURE
-----------------	--------------------	--------------------------------

FIGURE 12: Working Drawing of Center Point Micro Bending Fixture

2 POINT MICRO-  
BENDING FIXTURE

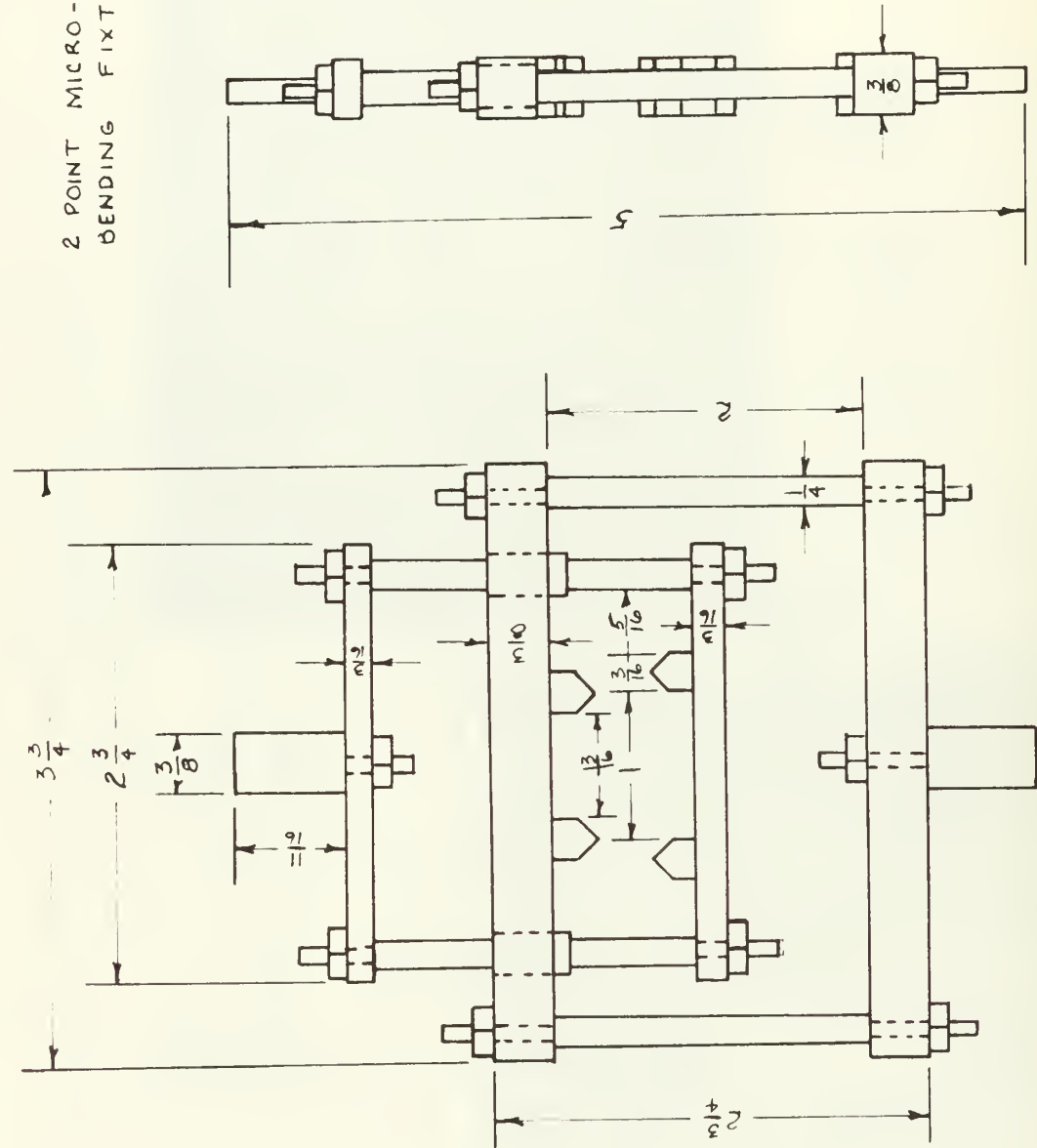


FIGURE 13: Working Drawing of Two Point Micro Bending Fixture

SPLIT FURNACE FOR INSTRON MACHINE

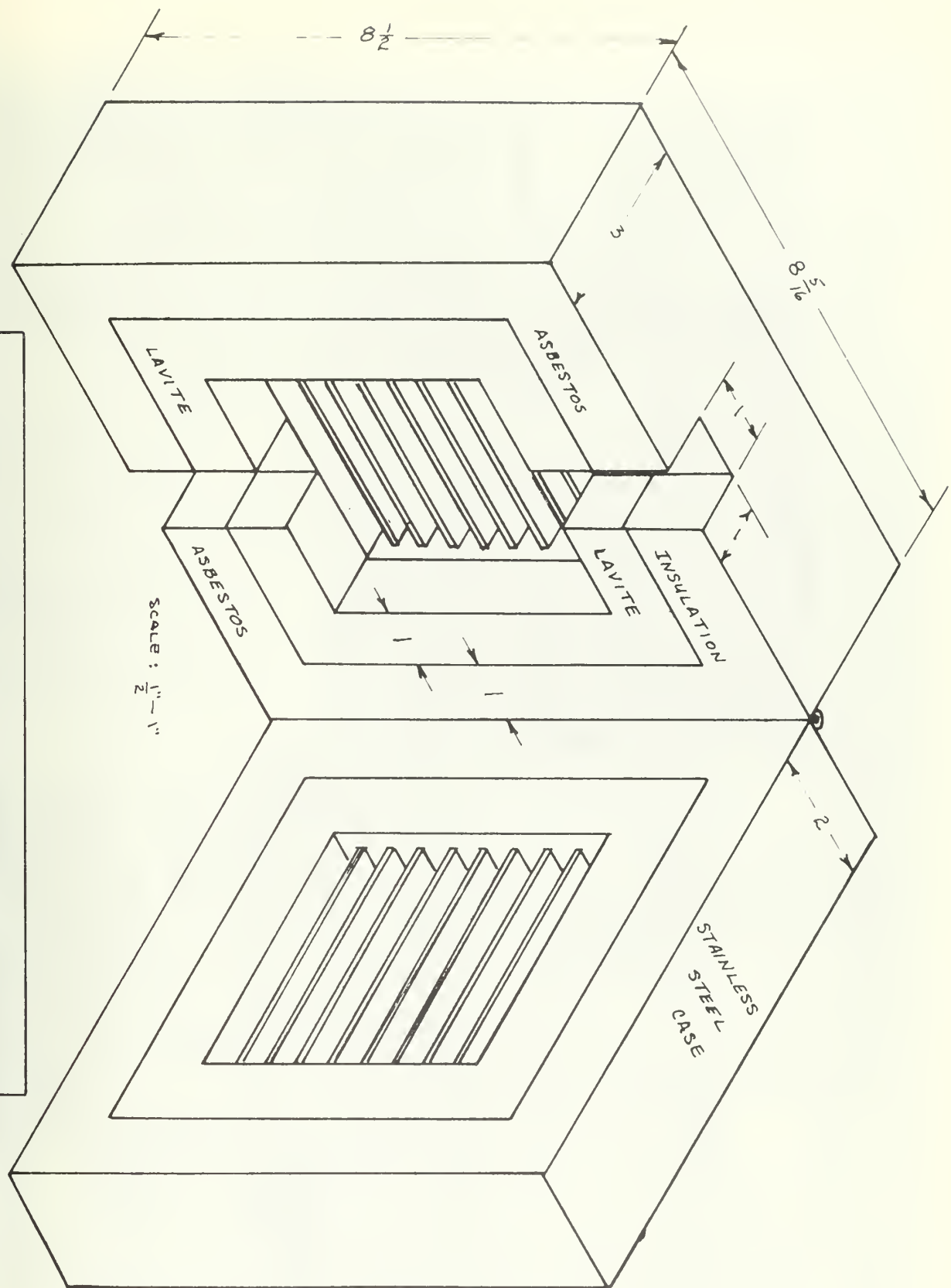


FIGURE 14: Working Drawing of Split Furnace for Instron Machine

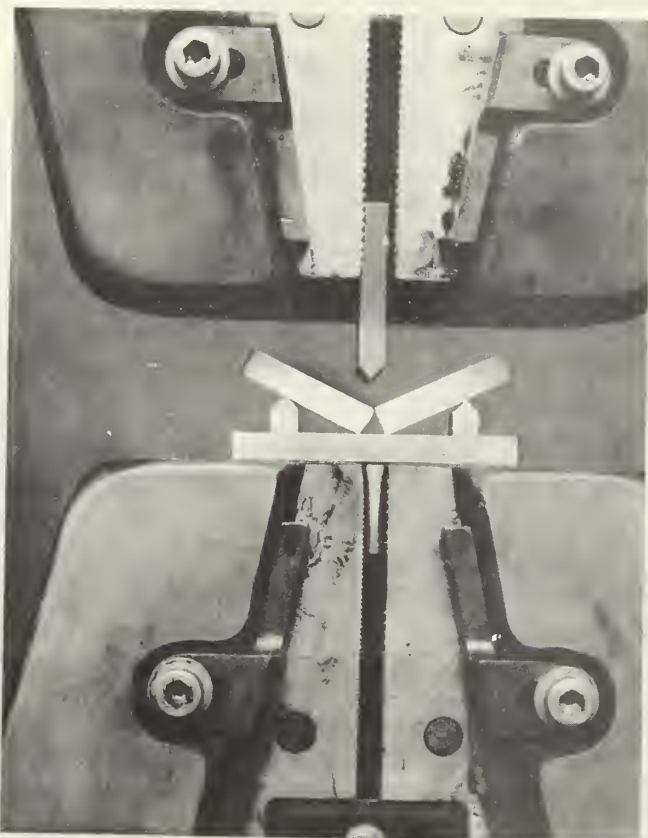


FIGURE 15

Re-designed Center Point Micro Bending Fixture as Assembled on Instron Tester.



FIGURE 16

Re-designed Two Point Micro Bending Fixture as Assembled on Instron Tester

FIGURE 19  
View of Uncoated and Coated Molybdenum  
Specimen (seen from Right to Left)

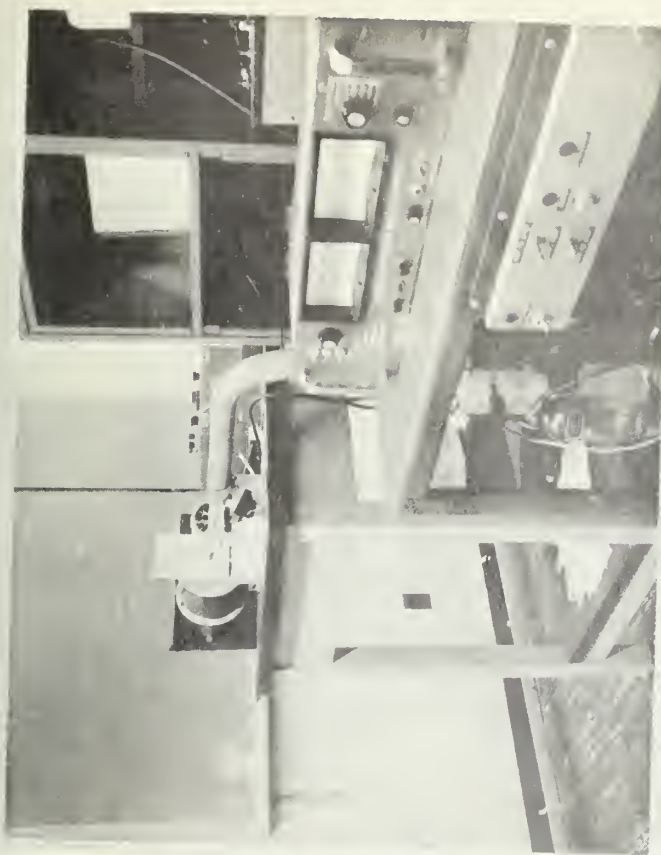
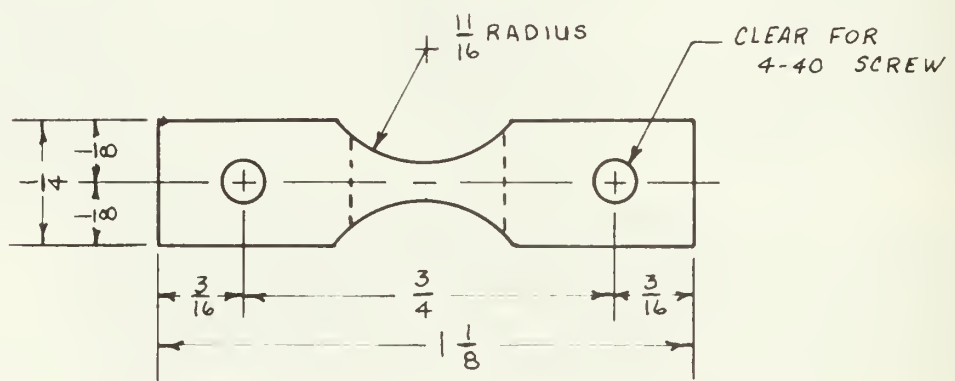
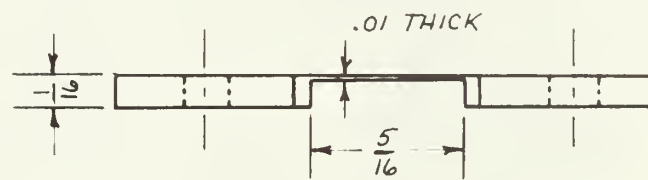


FIGURE 17  
View Showing Vacuum Stability Experiment  
Set-Up.





SCALE: NOT TO SCALE  
MAT'L: MOLYBDENUM

OHMIC HEATING SPECIMAN  
DRN. BY: B. ROBERTS

FIGURE 18: Working Drawing of Ohmic Heating Specimen

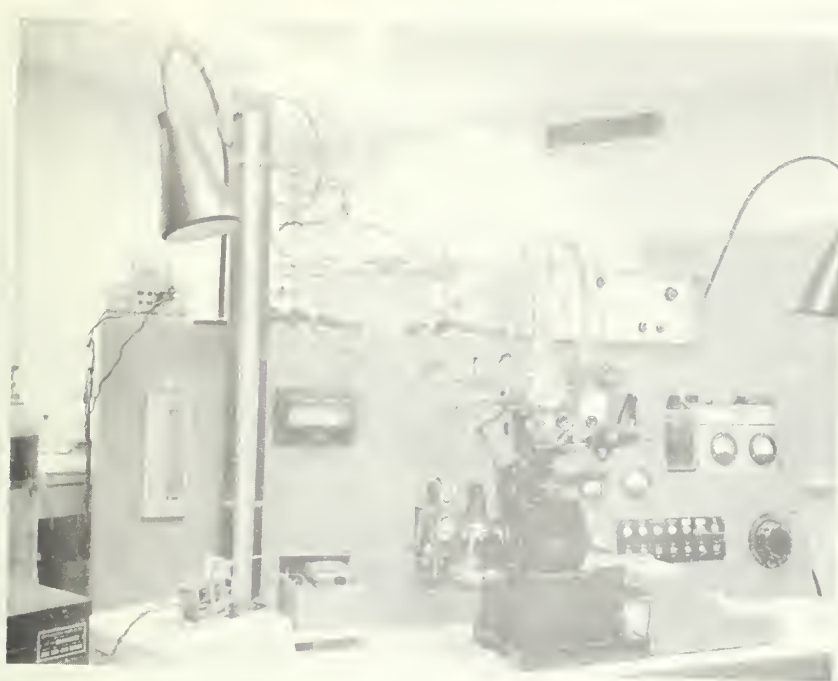


FIGURE 20

High Temperature Solid State Phenomenon  
Demonstrator.

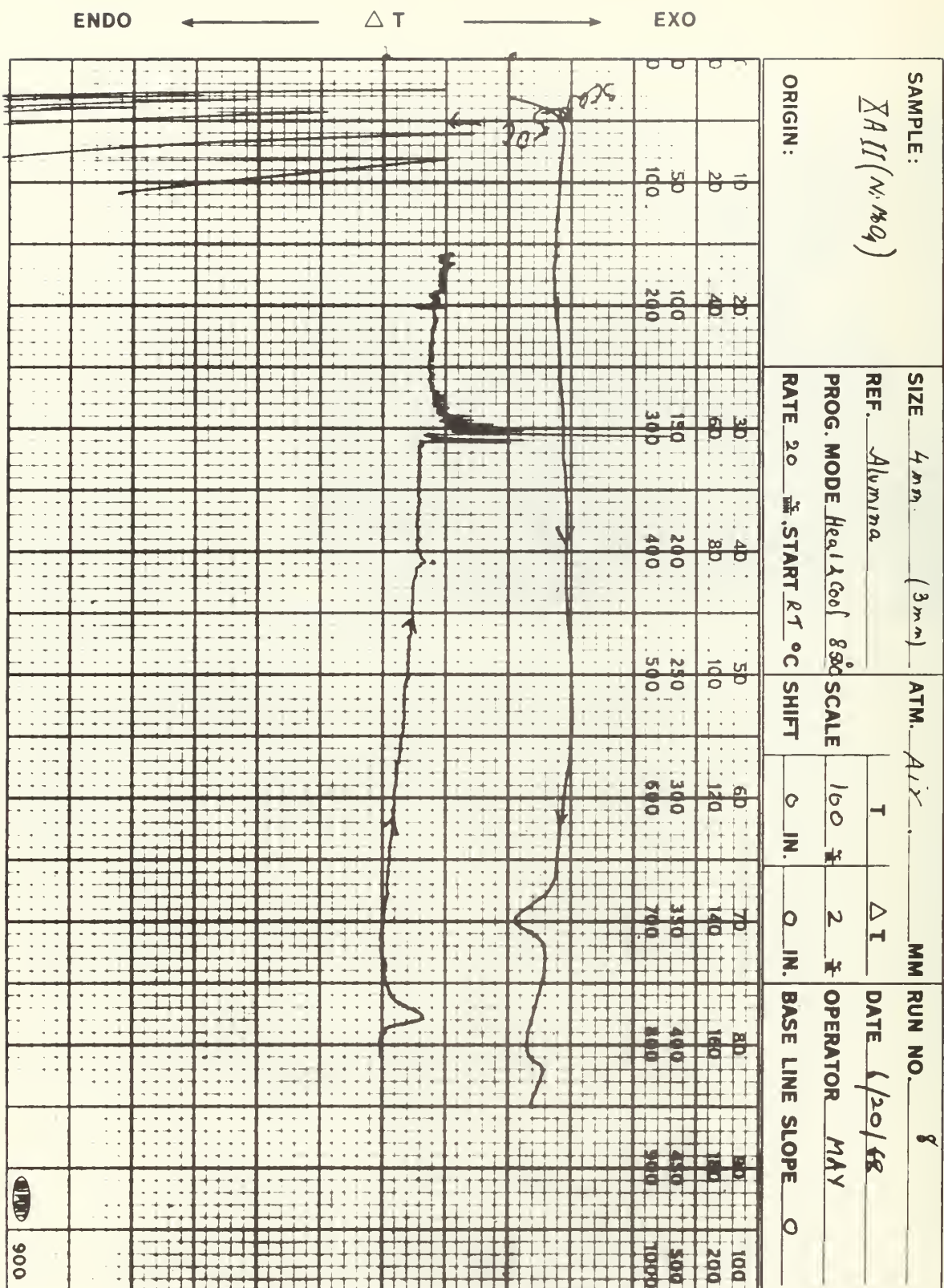


FIGURE 21: Thermogram of Nickel Molybdate

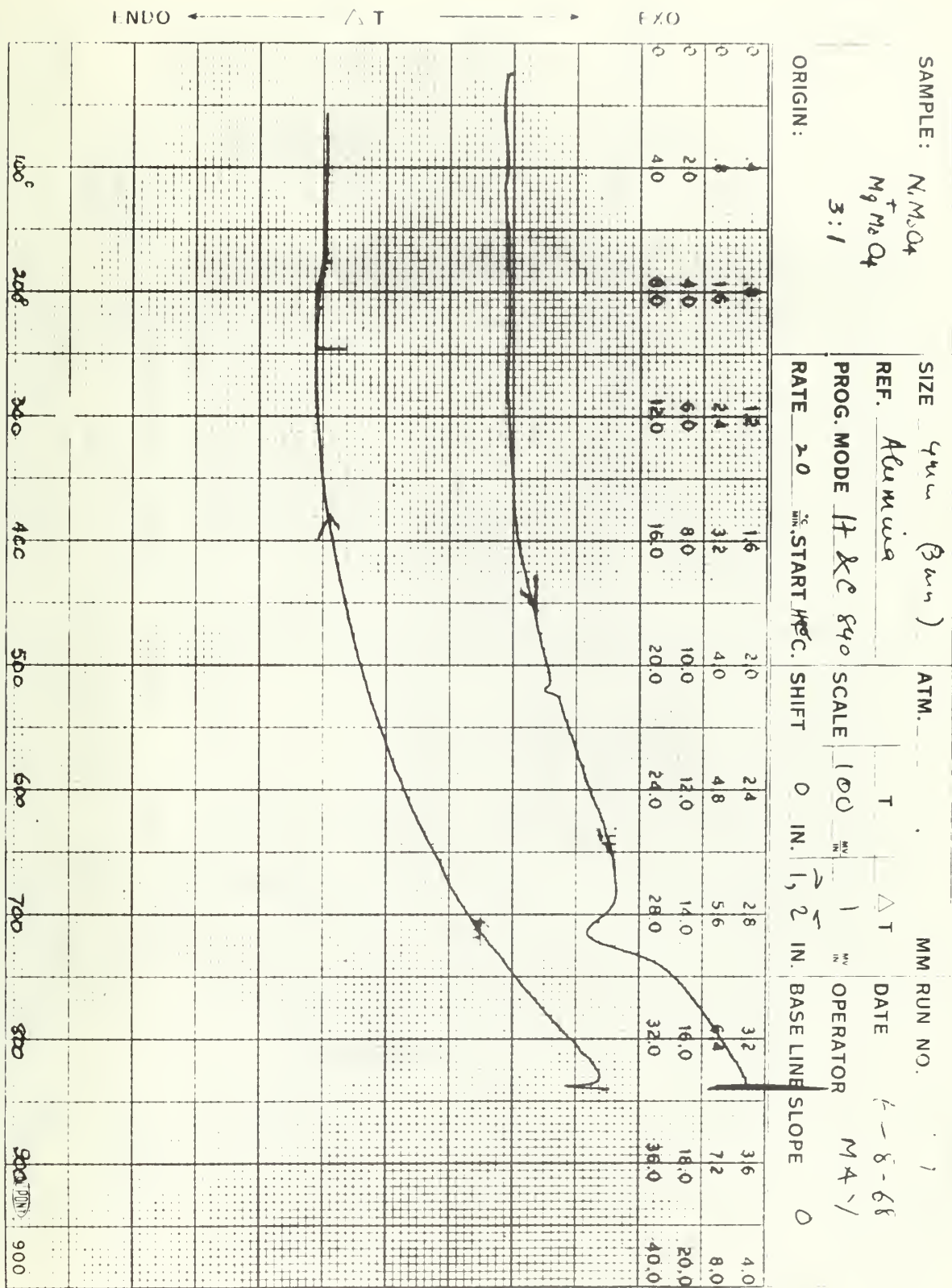


FIGURE 22: Thermogram of Nickel and Magnesium Molybdates Solid Solution 3:1

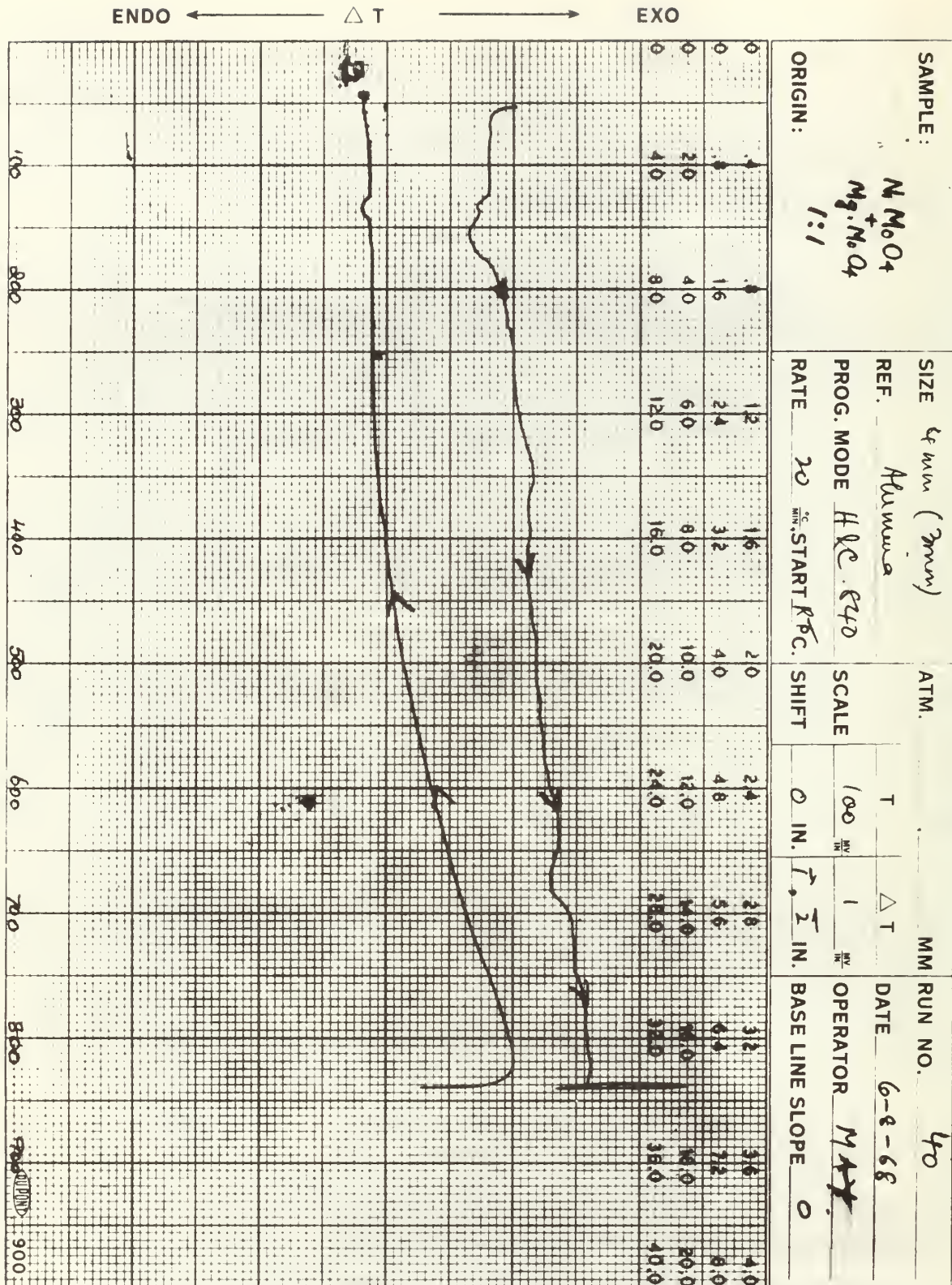
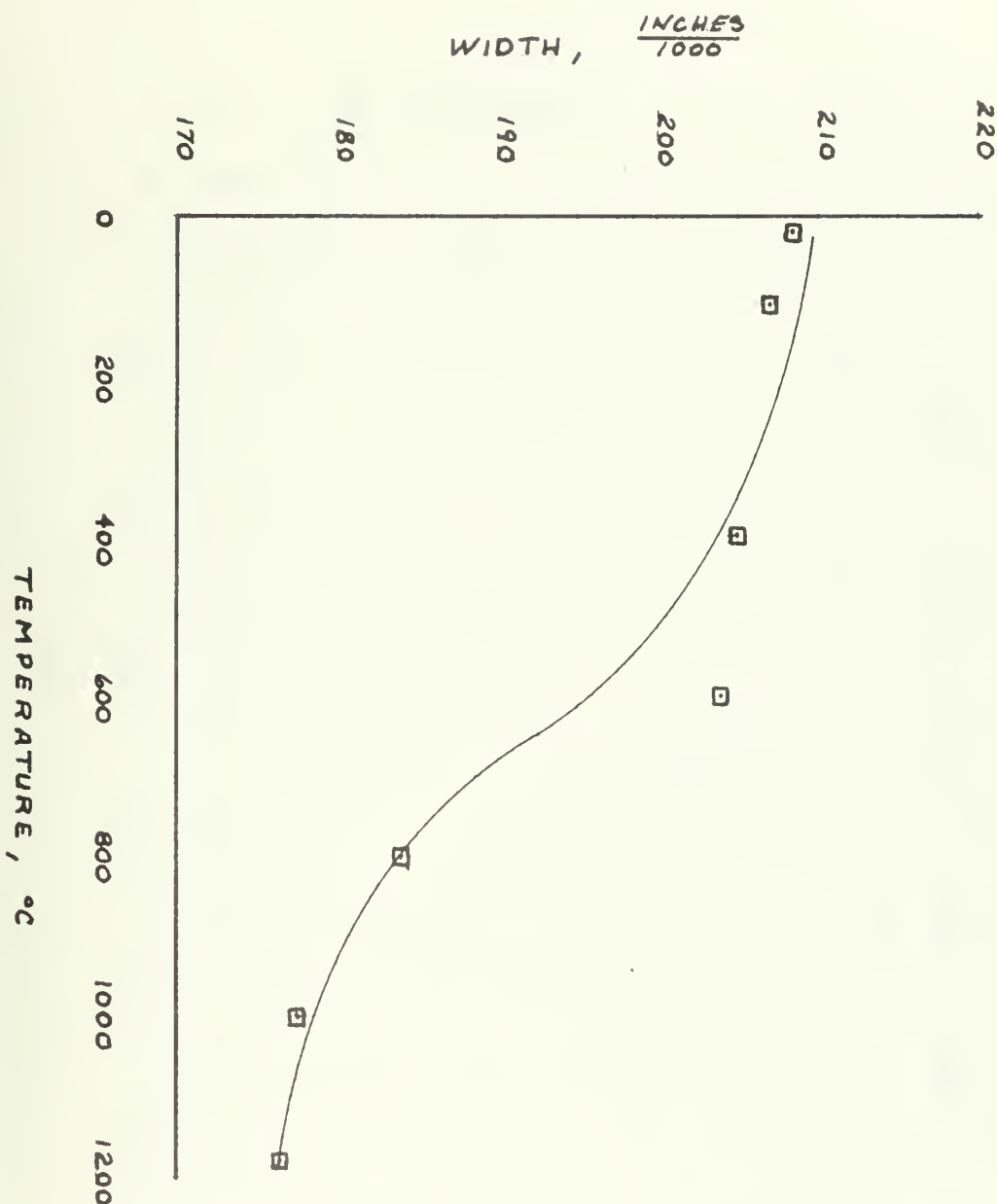


FIGURE 23: Thermogram of Nickel and Magnesium Molybdates Solid Solution 1:1



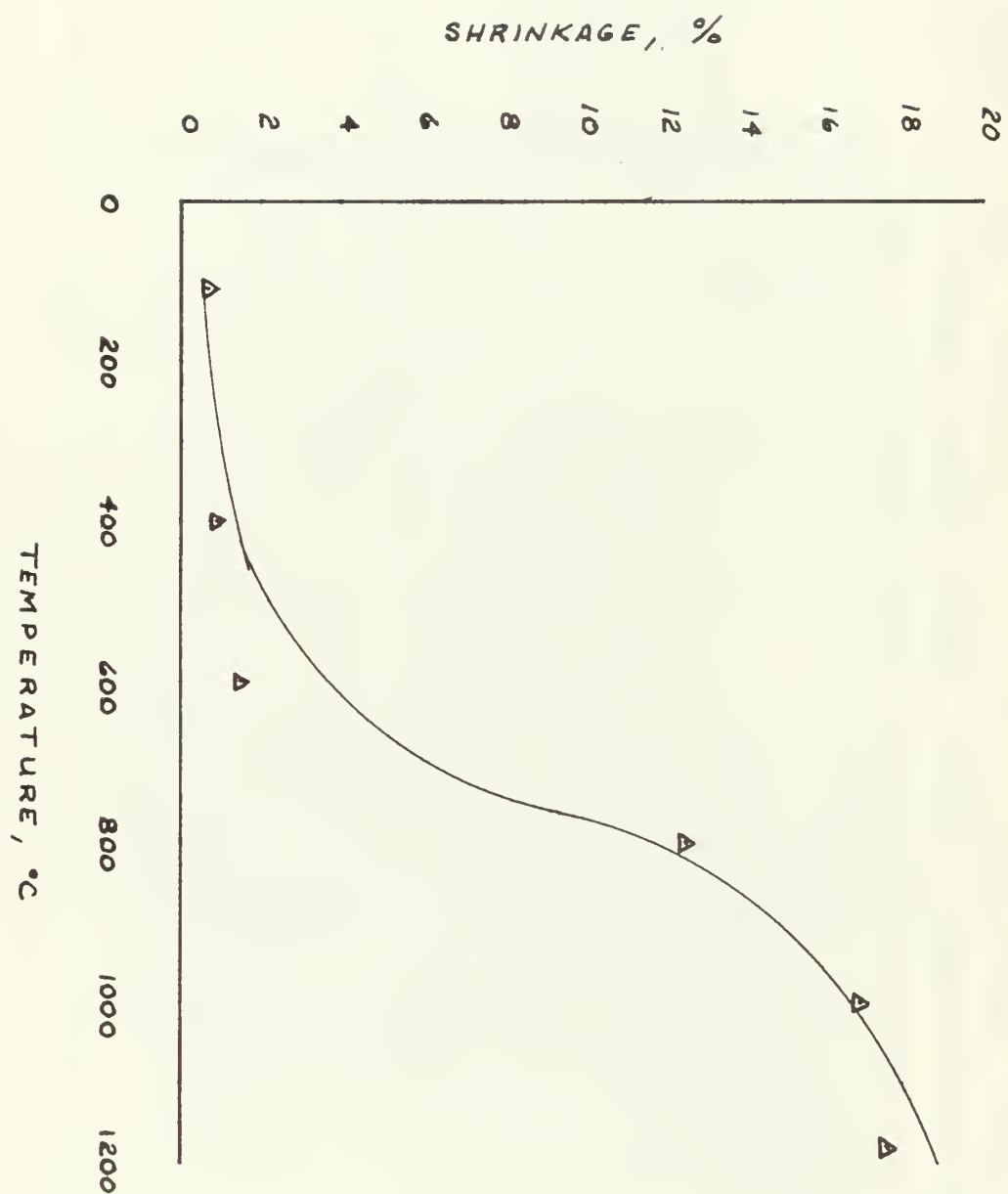


FIGURE 25: Variation of % Shrinkage with Temperature for Magnesium Molybdate Specimen molded Under 18,500 psi.

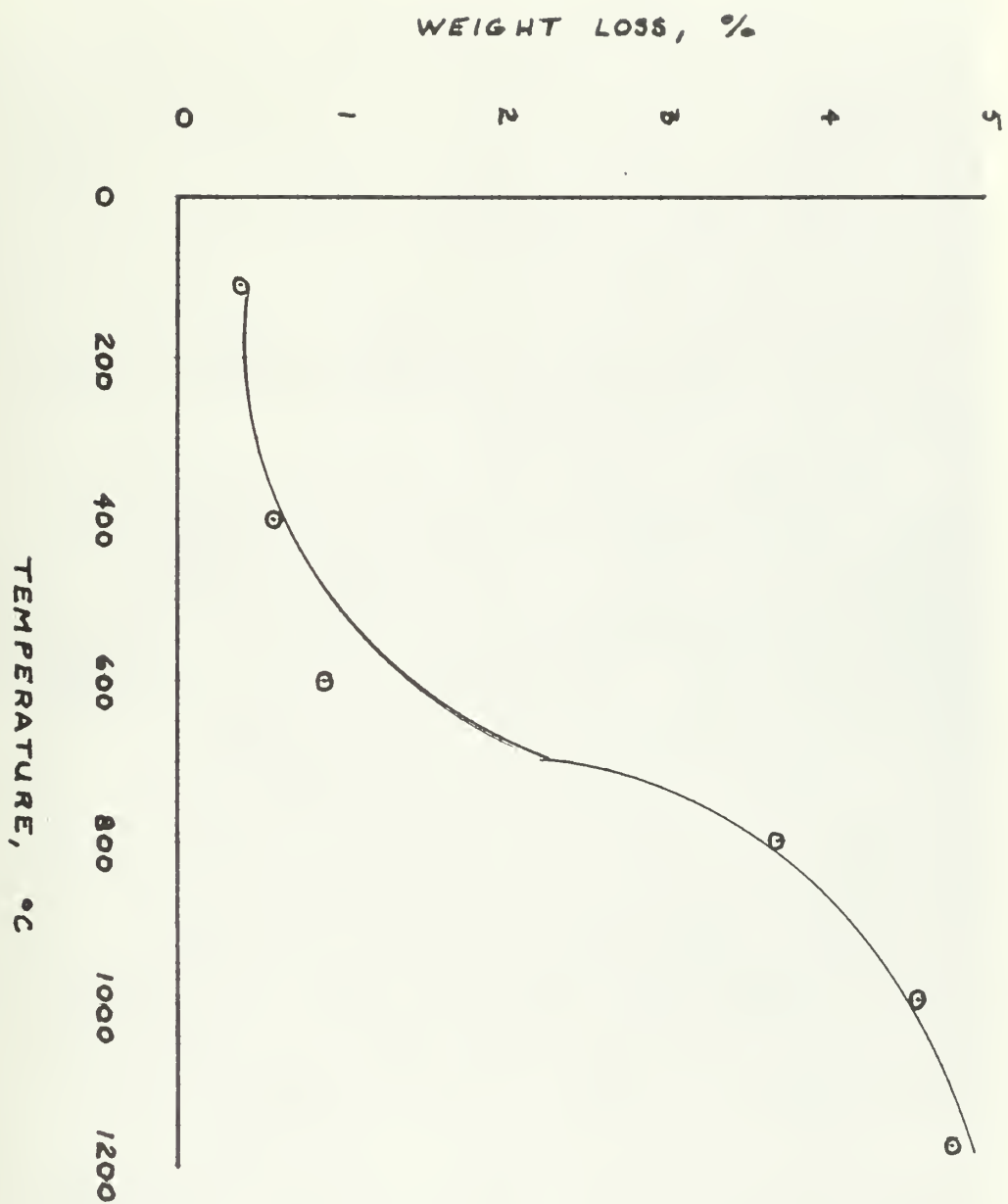


FIGURE 26: Variation of % Loss in Weight with Temperature for Magnesium Molybdate Specimen Molded Under 18,500 psi.



FIGURE 27: Coated Surface of Specimen at 250°C Showing Circular Drop Like Pattern Growth 500 X After Enlargement.



FIGURE 28: Coated Surface of Specimen at 900°. Further Nucleation of Oxide Indicated by the Crack in the Upper Right-hand Corner. 500 X After Enlargement

## BIBLIOGRAPHY

1. Kofstad, P.,  
High-Temperature Oxidation of Metals  
John Wiley and Sons, Inc., New York (1966)
2. Uhlig, H. H.,  
Corrosion and Corrosion Control  
John Wiley and Sons, Inc., New York (1963)
3. Hauffe, K.,  
Oxidation of Metals  
Plenum Press, New York (1965)
4. Evan, U. R.,  
The Corrosion and Oxidation of Metals  
St. Martins Press, Inc., New York (1960)
5. Krier, C. A.,  
Coatings for the Protection of Refractory Metal from Oxidation  
DMIC Report 162 (Nov. 1961)
6. Huminik, J.,  
High Temperature Inorganic Coatings  
Reinhold Publishing Corporation, New York (1963)
7. Kubaschewski, O., and Hopkins, B. E.,  
Oxidation of Metals and Alloys  
Butterworths, London, (1962)
8. Modisette, J. L. and Schryer, D. R.,  
"An Investigation of the Role of Gaseous Diffusion in the Oxidation  
of a Metal Forming a Volatile Oxide"  
NASA TND-222 (March 1960)
9. E. A. Gulbransen, Andrew, K. F., and Brassart, F. A.,  
Oxidation of Mo at 550 to 1700°C  
Scientific paper 62-123-121-Ps  
Westinghouse Research Labs., 1962
10. Lustman, B.,  
Metal Progress  
57(1950) 5.
11. Bartlett, E. S., and Williams, D. N.,  
Trans AIME, 212 (1958), 280.
12. Jones, E. S., Mosher, J. F., Speiser, R., and Sprentnak, J. W.,  
Corrosion, 14 (1958) 2t
13. Semmel, J. W., Jr.,  
High Temperature Materials  
AIME Conference

14. Wilks, C. R.,  
"Effect of Temperature, Pressure and Mass Flow on Oxidation of Molybdenum"  
paper presented to the SAMPE Estern Division Meeting  
Krege Hall, M.I.T. (May 1960)
15. LaChance, M. H., and Jaffee R. I.,  
"Fabrication and Evaluation of Thin Clad Sheets of Molybdenum"  
Trans. Asm 48, 595 (1956)
16. Preece, A., and Lucas, G.,  
"The High Temperature Oxidation of Cobalt-Base and Mickel Bas Alloys"  
J. Inst. Met. 81, 219 (1952-53)
17. Brenner, S. S.,  
"Oxidation of Iron Molybdenum and Mickel-Molybdenum Alloys"  
J. Electro Chem. Soc. 102 16(1955)
18. Rathenau, G. W., and Meijering, J. L.,  
"Rapid Oxidation of Metals and Alloys in the Presence of  $MoO_3$ "  
Metallurgia, 42 167 (1950)
19. Leslie, W. C., and Fontana, M. G.,  
"Mechanism of the Rapid Oxidation of High Temperature High Strength Alloys Containing Molybdenum"  
Trans Asm 41, 1213 (1949)
20. Monkman, F. C., and Grant, N. J.,  
"An Investigation of Accelerated Oxidation of Heat Resistant Metals Due to Vanadium"  
Corrosion, 9, 460 (1953)
21. Larsen, W. L.,  
"The Oxidation and Oxidation of Molybdenum -- Nickel Alloys"  
Ph. D. Thesis, Ohio State University 1956
22. Brasunas A. deS., and Grant N. J.,  
"Accelerated Oxidation of Metals at High Temperatures"  
Trans. AMA. 44, 1117 (1952)
23. Brenner, S. S.,  
"Catastrophic Oxidation of Some Molybdenum Containing Alloys"  
J. Electro Chem. Soc., 102, 16 (1955)
24. Gleiser, M., Larsen, W. L., Speiser, R., and Spretnak, J. W.,  
"The Properties of Oxidation - Resistant Scales Formed on Molybdenum - Base Alloys at Elevated Temperatures"  
A.S.T.M. Special Technical Publications No. 171, p. 65 (1955)
25. Kingerey, W. D.,  
"High Temperature Technology"  
Proceedings of an International Symposium at Asilomar, California  
McGraw-Hill, New York (1960)

26. Bartlett, E. S., Ogden, H. R., and Jafee, R. T.,  
"Coatings for Protecting Molybdenum from Oxidation at Elevated  
Temperatures"  
DMIC Report No. 109 (March 1959)
27. Rhys, D. W.,  
"Laboratory Studies of Processes Using Platinum for the  
Protection of Molybdenum Against Oxidation at High Temperatures"  
Comptes rendu du Sympsium sur la Fusion du Verre, Bruxelles (1958)
28. Levinstein, M. A. and Wlodek, S. T.,  
The Science and Technology of Molybdenum, Tungsten, Niobium, Tantalum  
and Their Alloys.  
Butterworths, London 1964
29. Todd, G. and Parry, E.  
Nature, 203 (1964), 967
30. Perkins, R. A.  
"Material Science and Technology for Advanced Applications"  
Vol II (1964, Golden Gate Metal's Conference, San Francisco 1964)
31. Fitzer, E.  
Plansee Proc., 1955, Reutte/Tyrol, 1956, 56.
32. Smith, G. W.  
Acla Cryst, 15, 1054 (1962)
33. Smith, G. W. and Ibers, J. A.  
Lbid, 19, 269 (1965)
34. Abraham, S. C., and Reddy, J. M.  
J. Chem. Phys 43, 2533 (1955)
35. Abraham, S. C.  
Acta Cryst, 21 Suppl, A40 (1966)
36. Abraham, S. C.  
J. Chem. Phys, 46, 2052 (1967)
37. Abraham, S. C., and Bernstein, J. L., and Jamieson, P. B.  
J. Chemical Physics 48, 2619 (1968)
38. Carlston, R. C.  
Norelco Reports, 10, 8(1963)
39. Young, A. P., and Schwartz, C. M.  
Science, 141, 348(1963)
40. Keeling, R. O.,  
Acta Cryst, 10, 209 (1957)

41. Carlston, R. C., Rodier, D.,  
Grumman Res. Dept. Memo RM-209, March 1964  
available from CFSTI as AD475571
42. Ward, R.  
Mixed Metal Oxides  
Progress in Inorganic Chemistry, 1, 465 (1959)  
edited by F. D. Cotton, Interscience N. Y.
43. Uitert, L. G. Van., Rubin, J. L., and Bonner, W. A.  
J. Am Ceramic Soc 46, 512(1963)
44. Doyle, W. P., Guire, G. Mc., Clark, G. M.  
J. Inorg and Mat. Chem 1185 ( )
45. Broch, E. K.  
Skynorske Vidensk Akad. Mat. Nat. Klasse  
No. 8(1929)
46. Kindig, J. N.,  
Thesis: Development of Equipment and Procedures for the  
Microscopic Observation of Selected Oxidation Processes.  
Maval Postgraduate, School, Monterey, California, June 1967
47. Wolfhard, H. G., Glassman, I., and Green, L. Jr., Editors  
Hetrogeneous Combustion, Progress in Astronautics and Aeronautics  
Vol 15, Academic Press, New York, pp 1-307 (1964)
48. King, B. W., et al.,  
"Nature of Adherance of Porcelain Enamels to Metals"  
J. Am. Ceramic Soc., 42, No. 11, 504(1959)
49. Jones, E. S., and Jahnke, L. P.,  
"Updating High-Temperature Metallurgy"  
Metal Progress, 78 (4) 131-135 (Oct 1960)
50. Jaffee, R. I. and Maykuth, D. J.,  
"Refractory Materials"  
DMIC Memorandum 44 (February 1960)

INITIAL DISTRIBUTION LIST

	No. Copies
1. Defense Documentation Center Cameron Station Alexandria, Virginia 22314	20
2. Library Naval Postgraduate School Monterey, California	2
3. Commander Naval Air Systems Command Hqs. Washington, D. C. 20360	1
4. Commander Naval Ordnance Systems Command Hqs. Washington, D. C. 20360	1
5. Professor G. F. Kinney Department of Chemistry and Material Science Naval Postgraduate School Monterey, California	5
6. Dr. R. C. Carlston Department of Chemistry and Material Science Naval Postgraduate School Monterey, California	3
7. Commander M. A. Yehya Defence Science Laboratories 34 - 37 P.N.H. Lines Karachi - Pakistan	3
8. Naval Attache Embassy of Pakistan 2315 Massachusetts Avenue, N.W. Washington, D. C. 20008	3

## UNCLASSIFIED

Security Classification

## DOCUMENT CONTROL DATA - R &amp; D

Security classification of title, body of abstract and indexing annotation must be entered when the overall report is classified)

ORIGINATING ACTIVITY (Corporate author) Naval Postgraduate School Monterey, California 93940	2a. REPORT SECURITY CLASSIFICATION Unclassified
	2b. GROUP N/A

## REPORT TITLE

Oxidation Protection of Molybdenum by Divalent Metal Molybdates

## DESCRIPTIVE NOTES (Type of report and, inclusive dates)

Thesis

## AUTHOR(S) (First name, middle initial, last name)

Mohammed Akhtar Yehya

REPORT DATE December 1968	7a. TOTAL NO. OF PAGES 70	7b. NO. OF REFS 50
CONTRACT OR GRANT NO.	9a. ORIGINATOR'S REPORT NUMBER(S)	
PROJECT NO.	9b. OTHER REPORT NO(S) (Any other numbers that may be assigned this report)	

## DISTRIBUTION STATEMENT

This document has been approved for public release and sale; its distribution is unlimited.

SUPPLEMENTARY NOTES N/A	12. SPONSORING MILITARY ACTIVITY Naval Postgraduate School
----------------------------	---

## ABSTRACT

Ni and Mg molybdates were prepared by an aqueous process and identified by x-ray analysis. Differential Thermal Analysis (DTA) of molybdates and their solid solutions mixed at various proportions were carried out. The spalling of  $\text{NiMoO}_4$  on cooling was observed. This large exothermic phase transformation was modified. Flexural strength of  $\text{MgMoO}_4$  bars were determined. Furnace designed to carry out this test at elevated temperature Vacuum Stability of bars made of  $\text{NgMoO}_4$  at high temperatures was observed. Slurry process of coating Molybdenum was carried out with some success and the same sintered at  $950^{\circ}\text{C}$  in high vacuum. An attempt was made to study the coated material at high temperatures under high vacuum and desired controlled atmosphere by a metallograph.

## Security Classification

14 KEY WORDS	LINK A		LINK B		LINK C	
	ROLE	WT	ROLE	WT	ROLE	WT

DD FORM 1473 (BACK)

1 NOV 65  
S/N 0101-002-6801















thesY34

Oxidation protection of molybdenum by di



3 2768 001 90508 6  
DUDLEY KNOX LIBRARY